

Calibrating the metallicity of M dwarfs in wide physical binaries with F-, G-, and K- primaries – I: High-resolution spectroscopy with HERMES: stellar parameters, abundances, and kinematics*

D. Montes¹†, R. González-Peinado¹, H. M. Tabernero^{2,1}, J. A. Caballero³, E. Marfil¹, F. J. Alonso-Floriano^{4,1}, M. Cortés-Contreras³, J. I. González Hernández^{5,6}, A. Klutsch^{7,1}, and C. Moreno-Jódar^{8,1}

¹Departamento de Física de la Tierra y Astrofísica & UPARCOS-UCM (Unidad de Física de Partículas y del Cosmos de la UCM), Facultad de Ciencias Físicas, Universidad Complutense de Madrid, E-28040 Madrid, Spain

²Departamento de Física, Ingeniería de Sistemas y Teoría de la Señal, Universidad de Alicante, Apdo. 99 E-03080, Alicante, Spain

³Centro de Astrobiología (INTA-CSIC), ESAC campus, Camino Bajo del Castillo s/n, E-28691 Villanueva de la Cañada, Madrid, Spain

⁴Leiden Observatory, Leiden University, 2300 RA Leiden, Netherlands

⁵Instituto de Astrofísica de Canarias (IAC), Calle Vía Láctea s/n, E-38200 La Laguna, Tenerife, Spain

⁶Departamento Astrofísica, Universidad de La Laguna, E-38206 La Laguna, Tenerife, Spain

⁷INAF - Osservatorio Astrofisico di Catania, via S. Sofia 78, 95123 Catania, Italy

⁸Escuela Técnica Superior de Ingeniería Aeronáutica y del Espacio, Plaza de Cardenal Cisneros 3, E-28040, Madrid, Spain

Accepted 2018 May 09. Received 2018 May 09; in original form 2018 March 02

ABSTRACT

We investigated almost 500 stars distributed among 193 binary or multiple systems made of late-F, G-, or early-K primaries and late-K or M dwarf companion candidates. For all of them, we compiled or measured coordinates, *J*-band magnitudes, spectral types, distances, and proper motions. With these data, we established a sample of 192 physically bound systems. In parallel, we carried out observations with HERMES/Mercator and obtained high-resolution spectra for the 192 primaries and five secondaries. We used these spectra and the automatic STEPAR code for deriving precise stellar atmospheric parameters: T_{eff} , $\log g$, ξ , and chemical abundances for 13 atomic species, including [Fe/H]. After computing Galactocentric space velocities for all the primary stars, we performed a kinematic analysis and classified them in different Galactic populations and stellar kinematic groups of very different ages, which match our own metallicity determinations and isochronal age estimations. In particular, we identified three systems in the halo and 33 systems in the young Local Association, Ursa Major and Castor moving groups, and IC 2391 and Hyades Superclusters. We finally studied the exoplanet-metallicity relation in our 193 primaries and made a list 13 M-dwarf companions with very high metallicity that can be the targets of new dedicated exoplanet surveys. All in all, our dataset will be of great help for future works on the accurate determination of metallicity of M dwarfs.

Key words: proper motions – stars: abundances – binaries: visual – stars: fundamental parameters – stars: late-type – stars: solar-type

1 INTRODUCTION

Cool, low-mass dwarfs of M spectral type are, by far, the most numerous stellar constituents of the Milky Way. Having main-sequence lifetimes that exceed the current age of the Universe

(Baraffe et al. 1998; Henry et al. 2006), M dwarfs stand as excellent objects in order to probe the structure and evolution of the Milky Way’s thin and thick discs. Because of their ubiquity, M dwarfs may also be the largest population of planet-hosting stars. As a result, a large fraction of low-mass planets are expected to orbit an M-type star within its habitable zone, which is considerably closer than for solar-like ones.

* Based on observations obtained with the HERMES spectrograph mounted on the 1.2 m Mercator Telescope at the Spanish Observatorio del Roque de los Muchachos of the Instituto de Astrofísica de Canarias

† E-mail: dmontes@ucm.es

More importantly, the detectability of any such planet via the transit and radial-velocity techniques is enhanced by the lower

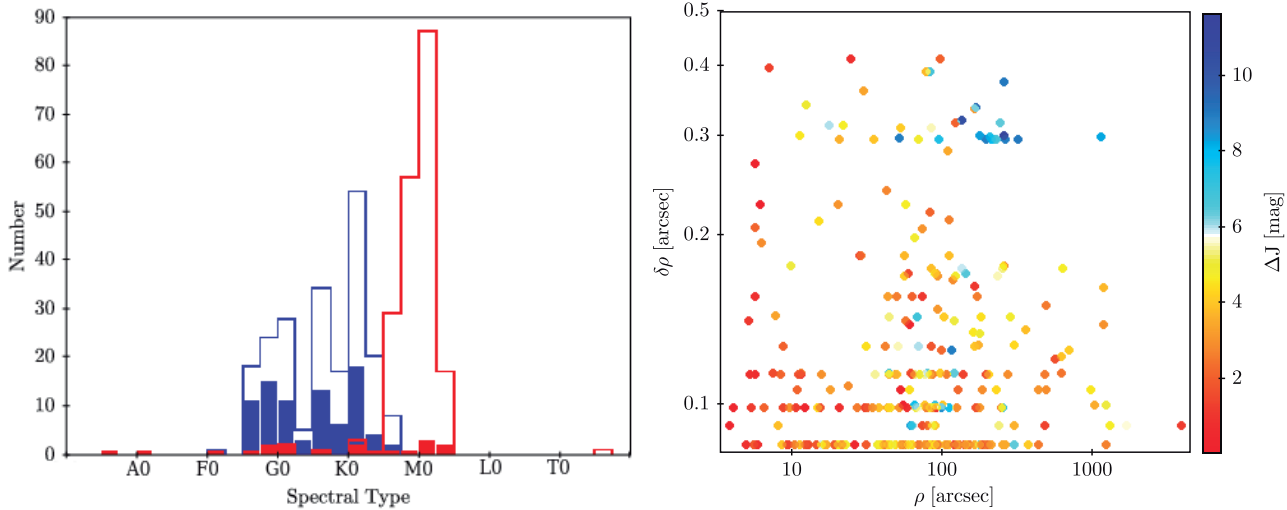


Figure 1. *Left panel:* distribution of spectral types for the stars of our sample. Blue and red bars represent primaries and secondary candidates, respectively, while open and filled bars represent physical and optical components, respectively. Note the tail of optical secondaries in the background with spectral types much earlier than primaries. The late T dwarf is GJ 570 D (Burgasser et al. 2000). *Right panel:* angular separation between stars in pairs and their uncertainties, colour-coded with the difference in J magnitude.

masses and smaller radii of M dwarfs (Clanton & Gaudi 2014; Reiners et al. 2018). Therefore, M dwarfs have become key targets for planet hunting (e.g. MEarth – Charbonneau et al. 2009; Berta-Thompson et al. 2015; Dittmann et al. 2017). This is also illustrated by new spectrographs optimised for exoplanet searches around M dwarfs (e.g. CARMENES – Alonso-Floriano et al. 2015a; Quirrenbach et al. 2016; Reiners et al. 2018).

The observational efficiency of exoplanet searches around M dwarfs could be vastly increased with prior knowledge of stellar metallicity. In this sense, previous studies have already pointed out that planets are more likely to be found orbiting metal-rich, solar-like stars (Santos et al. 2001, 2004; Fischer & Valenti 2005 – but see below). However, the metallicity of low-mass dwarfs has been an elusive fundamental property due to the complexity of modeling their atmospheres. Fortunately, the advent of new observational techniques, as well as independent theoretical improvements in atmospheric models, now seem to link the metallicity of M dwarfs to both their photospheric and spectroscopic features (Bonfils et al. 2005; Bean et al. 2006b; Woolf & Wallerstein 2006; Johnson & Apps 2009; Hauschildt & Baron 2010; Rojas-Ayala et al. 2010, 2012; Önehag et al. 2012; Neves et al. 2014; Maldonado et al. 2015; Passegger et al. 2018). Not only do these metallicity studies have deep implications in the realm of stellar astrophysics, but they also play a crucial role in the analysis of the Galactic evolution (West et al. 2011; Woolf & West 2012).

There were preliminary indications that the M dwarfs with known planets have sub-solar metallicities (Bonfils et al. 2005; Bean et al. 2006b), in contrast to their earlier counterparts. Actually, while giant planets preferentially form around metal-rich stars, Neptunes and super-Earths are not necessarily more abundant in metal-rich stars but they are abundant at solar metallicity (Sousa et al. 2008; Adibekyan et al. 2012; Buchhave et al. 2012). However, more recent results showed instead that planet-hosting M dwarfs appear to be metal-rich (Johnson & Apps 2009; Rojas-Ayala et al. 2010; Terrien et al. 2012). We refer the reader to Hobson et al. (2018) for a recent review on the planet-metallicity relation in M dwarfs.

A few studies have estimated M-dwarf metallicities using wide multiple systems that consist of at least an M dwarf and a higher-mass star, typically of late F-, G-, or early-K spectral type. Since binaries are assumed to be born in a common parental cloud and be coeval, the composition of the FGK star, which can be accurately derived from a careful comparison with theoretical models and current tools, can be extrapolated to its companion M dwarf. However, in some cases small differences in composition between components (often at a level of ≈ 0.05 dex) may arise if they are comoving but not coeval, there originally was chemical heterogeneity within the birth cloud, or some of the components underwent accretion of planetary material after birth (see Desidera et al. 2004; Teske et al. 2015; Brewer et al. 2016; Andrews et al. 2018; Oh et al. 2018, and references therein). Some of these studies have used optical and infrared spectroscopy to tie spectroscopic features to a metallicity scale (Valenti et al. 1998; Woolf & Wallerstein 2005, 2006; Bean et al. 2006a,b; Woolf et al. 2009; Rojas-Ayala et al. 2010, 2012; Terrien et al. 2012; Mann et al. 2013, 2014, 2015; Gaidos & Mann 2014; Newton et al. 2014; Souto et al. 2017). Other studies have used photometric calibrations. For example, Bonfils et al. (2005) and Johnson & Apps (2009) used M dwarfs in wide binaries to derive a relation between metallicity, absolute K -band magnitude, and the $V - K$ colour index (higher metallicity M dwarfs are slightly brighter at a given colour – see also Casagrande et al. 2008; Schlaufman & Laughlin 2010; Johnson et al. 2012; Neves et al. 2012).

To date, different authors with different methods have analysed only slightly over one hundred wide FGK+M benchmark systems, which results in a lack of homogeneity in the literature. A larger and homogeneous sample of wide visual binaries and multiple systems covering a large range in metallicity and spectral type is needed to reduce the scatter of the current calibrations and to get a good calibration relationship that would be valid throughout the parameter space. Here we start a series of papers devoted to improve the spectroscopic calibration of the M-dwarf metallicity. In this first article, we present our sample with a total of nearly 500 stars, study the common proper motion of the multiple systems,

and derive stellar atmospheric parameters of the FGK “primaries” (T_{eff} , $\log g$, ξ , and chemical abundances for 13 atomic species).

2 ANALYSIS

First of all, we collected from the literature 193 binary or multiple system candidates formed by late-F, G-, or early K-type primaries and late-K or M-type secondaries observable from Calar Alto, in Southern Spain ($\delta > -23$ deg). The main sources used to gather our initial sample were searches for common proper motion companions (Gliese & Jahreiß 1991; Poveda et al. 1994, 2009; Simons et al. 1996; Tokovinin 1997; Gould & Chanamé 2004; Zapatero Osorio & Martín 2004; Caballero 2007, 2009; Lépine & Bongiorno 2007; Raghavan et al. 2010), as well as previous metallicity calibrations of M dwarfs based on photometric and/or spectroscopic data (see Section 1). The sample consists on 489 stars distributed in 193 binary or multiple candidate systems, from which 193 are late-F, G-, or early K-type primaries, and 296 are companion candidates.

Table B1 lists the surveyed systems studied in this paper. For each of the 296 pairs of primaries and companion candidates, we tabulate its number and discoverer code as provided by the Washington Double Star Catalog (WDS – Mason et al. 2001). To avoid including too many spurious sources in the analysis, we tabulate all components with designation A to D regardless of their WDS notes (such as “Proper motion or other technique indicates that this pair is non-physical”), and all the physical pair candidates regardless of their designation (e.g. GJ 570 D is component G in WDS, HD 211472 B is component T in WDS). We were not able to identify faint optical companions found in deep adaptive optics surveys (e.g. Lafrenière et al. 2007; Ehrenreich et al. 2010; Janson et al. 2013; Ammler-von Eiff et al. 2016) and the LDS 585 “D” companion of the system WDS 17050–0504 (according to WDS, LDS 585 “D” is a dubious double¹). Three pairs have no WDS entry, and are marked with “...” in the ‘Discoverer code’ field.

In Table B1 we also provide angular separation ρ and position angle θ measured by us with the Virtual Observatory tool TOPCAT (Taylor 2005) from Two-Micron All Sky Survey (2MASS – Skrutskie et al. 2006) data, Simbad’s star name, equatorial coordinates, J -band magnitude, and spectral type from the literature. Fig. 1 shows the distribution of spectral types of primaries and companions. Most spectral types of primaries range from F4 V to K5 V, and of physical companions from K7 V to M7 V, while angular separations range from 4 to about 4000 arcsec, with uncertainties lower than 0.4 arcsec.

The close companion candidates in four systems with very bright primaries, namely WDS 04359+1631 (Aldebaran B), WDS 16147+3352 (σ CrB “C”), WDS 19553+0624 (β Aql B), and WDS 20462+3358 (ϵ Cyg B and C), were not tabulated by 2MASS in spite of being visible in their images. Besides, the 88-arcsec wide companion candidate BD–13 5608B in system WDS 20124–1237 was not tabulated by 2MASS due to a nearby speckle from the primary (ξ Cap). In these five cases, we computed ρ and θ with the raw 2MASS H -band images and Aladin Sky Atlas (Bonnarel et al. 2000).

¹ “A dubious double (or Bogus binary) may represent a positional typo in the original publication [...], an optical double disappearing due to radically different proper motions, a plate flaw, or simply a pair not at a magnitude, separation, etc., sufficiently similar to those noted when the first measure was added” (Mason et al. 2001).

In Table B2 we list heliocentric distances and proper motions of all the investigated stars, which we used for discarding optical (non-physical) pairs. First, we compiled parallactic distances in the following order from the Tycho–*Gaia* Astrometric Solution (TGAS – Gaia Collaboration et al. 2016), the new (HIP2 – van Leeuwen 2007) and old (HIP1 – Perryman et al. 1997) *Hipparcos* reductions, van Altena et al. (1995), and Prieur et al. (2014; only for μ^{O2} Her BC). All 193 primaries have parallactic distances, while only 52 companions do. Of the remaining 244 companion candidates, we derived our own spectro-photometric distances for 165 late K, and early and intermediate M dwarfs resolved by 2MASS, using the spectral type– M_J relation of Cortés-Contreras et al. (2017). As discussed in Section 4.2, this relationship is applicable only to main-sequence late-type dwarfs of solar metallicity, and the tabulated spectro-photometric distances of low-metallicity dwarfs must be handled with care. For two secondaries with J magnitude and reliable spectral type (η Cas B in WDS 00491+5749, and BD+48 3952B in WDS 23104+4901) we did not derive any distance because their 2MASS quality flags indicate a poor photometry. Besides, there are two physical companions, a white dwarf and a brown dwarf, with both spectral type and near-infrared magnitudes without a distance derived by us, namely σ^{O2} Eri B (DA2.3) in WDS J04153–0739, and GJ 570 D (T8) in WDS 14575–2125. Altogether, there are only 74 companion candidates without any heliocentric distance determination.

Next, we compiled proper motions for the 193 primaries and 293 (all but three) companions from the following catalogues and works: TGAS, Hot Stuff for One Year (HSOY – Altmann et al. 2017), HIP2, UCAC5 (Zacharias et al. 2017), Tycho-2 (Høg et al. 2000), PPMXL (Roeser et al. 2010), UCAC4 (Zacharias et al. 2012), Caballero (2009), Faherty et al. (2009, for GJ 570 D), and Ivanov (2008, for Aldebaran B), in this order. For 37 stars (36 secondaries and the primary 39 Leo A in WDS 10172+2306) with probably wrong proper motions or no proper motions whatsoever, we improved or measured their values for the first time. To do so, we used the method used by Caballero (2009) and the astrometric epochs from DENIS (Epchtein et al. 1997), USNO-A2 (Monet 1998), 2MASS, GSC2.3 (Lasker et al. 2008), AllWISE (Cutri & et al. 2014), CMC15 (Muñoz & Evans 2014), *Gaia* DR1 (Gaia Collaboration et al. 2016), and, in the most difficult cases, the SuperCOSMOS digitalization of the Digital Sky Survey photographic plates (Hambly et al. 2001). The time baseline varied between 4.5 and 119.3 years, with a median of seven astrometric epochs per star. As for the distances, we did not assign proper motions of primaries to companions. We were not able to compile or measure by ourselves any proper motions of the secondaries in the systems WDS 00491+5749 (η Cas AB; first measured in 1779), WDS 11378+4150 (BD+42 2230 AC; first detected in 1998) and WDS J21546–0318 (HD 208177 AB; first observed in 1829).

With the distances and proper motions in Table B2, we set a uniform criterion to distinguish between physical (bound) and optical (unbound) systems (Fig. 2, left panel). First, we computed two parameters for each pair of stars: the μ ratio, defined as:

$$(\mu \text{ ratio})^2 = \frac{(\mu_\alpha \cos \delta_1 - \mu_\alpha \cos \delta_2)^2 + (\mu_\delta 1 - \mu_\delta 2)^2}{(\mu_\alpha \cos \delta_1)^2 + (\mu_\delta 1)^2}, \quad (1)$$

and the proper motion position angle difference:

$$\Delta PA = |PA_1 - PA_2|, \quad (2)$$

where PA_i is the angle between $\mu_\alpha \cos \delta_i$ and $\mu_{\delta,i}$, being $i = 1$ for the primary star and $i = 2$ for the companion candidate.

We discarded 84 pairs of stars that have: (i) μ ratio > 0.15 ,

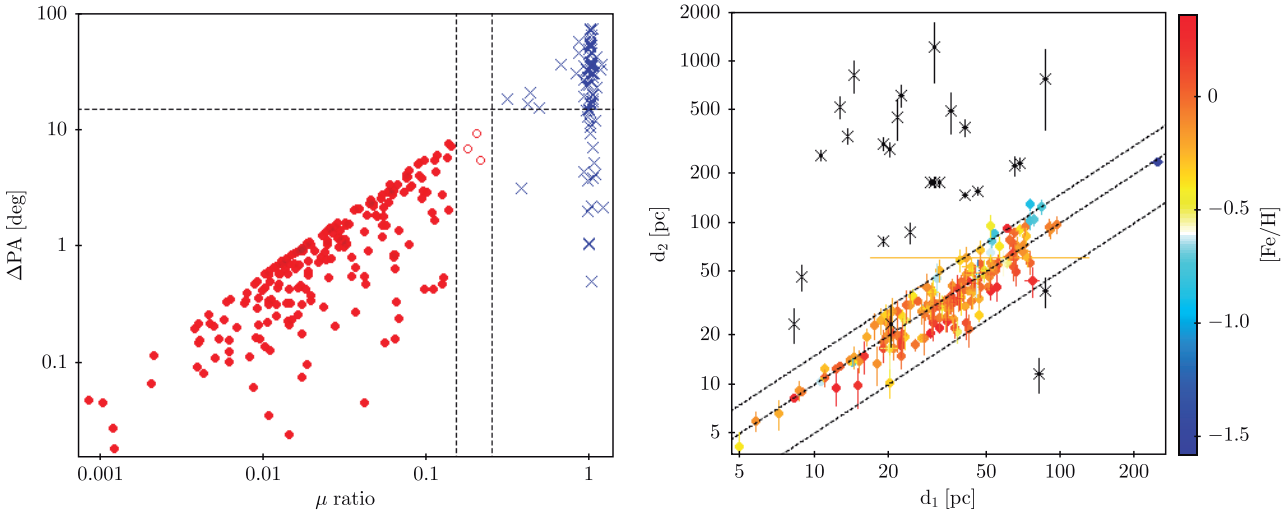


Figure 2. Left panel: ΔPA vs. μ ratio diagram. Physical (red filled circles), doubtful physical (red open circles) and optical (blue crosses) attending to our criteria. Dashed vertical and horizontal lines mark the 0.15 and 0.25 μ ratio and 15 deg ΔPA . Right panel: heliocentric distances for primary (1) and companion (2) stars colour-coded with metallicity. Dashed lines indicate 1.5:1, 1:1, and 0.5:1 d relationships, respectively. Black crosses represent optical pairs. Low-metallicity stars tend to lie in the upper part of the 1:1 distance relation.

and/or (ii) proper motion position angle difference $\Delta PA > 15$ deg (compare with the selection criteria in e.g. Lépine & Bongiorno 2007, Dhital et al. 2010, and Alonso-Floriano et al. 2015b). Besides, we investigated in detail the three pairs with $\Delta PA < 15$ deg and $0.15 < \mu$ ratio < 0.25 . Two of them, namely WDS 15282-0921 AC and WDS 23026+2948 AC, are very wide pairs ($\rho > 1000$ arcsec) that are affected by high proper motion projection effect (as between α Cen AB and Proxima). The third pair, WDS 23536+1207 AB (VYS 11), is a close binary of $\rho = 5.7$ arcsec already investigated by Tokovinin & Kiyaeva (2016). We also classified these three systems as physical despite they did not pass our μ ratio criterion. We must wait for *Gaia* DR2 to confirm them. Overall, we have 209 physical pairs distributed in 192 systems. We only discarded the source WDS 10585-1046 (LDS 4041).

As a double check, we compared the compiled and derived heliocentric distances of primaries and companions (Fig. 2, right panel). For systems with parallactic distances only, they vary less than 15 %, while for systems with spectro-photometric distances, they vary less than 50 %, except for three pairs with low metallicities (Section 4.2). To assure that we did not reject any physical pair because of abnormal metallicity, we did not discard any pair based on different heliocentric distances. New parallax-based distances, such as the ones provided by *Gaia* DR2 (Gaia Collaboration et al. 2018), are invaluable since they are independent of metallicity and stellar parameter analyses.

3 SPECTROSCOPY AND KINEMATICS

3.1 Observations and reduction

FGK-type stars of the multiple systems described above are relatively bright, $J < 9.0$ mag ($V < 11.0$ mag), which allowed us to obtain high signal-to-noise ratio, high-resolution, optical spectra with reasonable exposure times ($t_{\text{exp}} \leq 20$ min), and to derive reliable stellar parameters and abundances. We took high-resolution echelle spectra of 192 primaries and 5 secondaries with HERMES (High Efficiency and Resolution Mercator Echelle Spectrograph – Raskin et al. 2011) at the 1.2 m Mercator Telescope at the Observa-

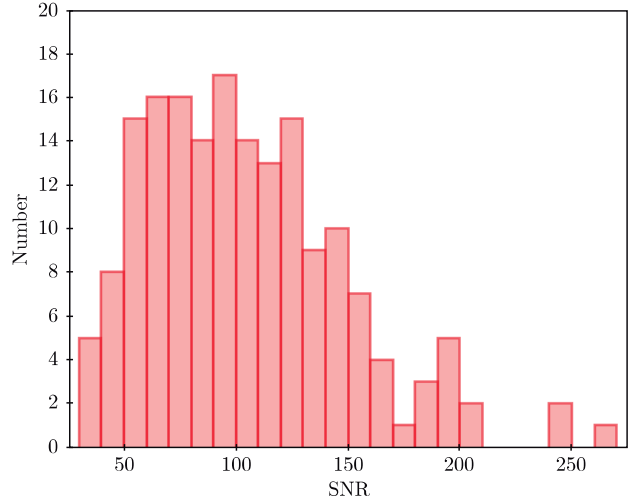


Figure 3. Histogram of signal-to-noise ratios measured in our HERMES spectra.

torio del Roque de los Muchachos (La Palma, Spain) between January 2010 and December 2017. We used the high resolution mode, which provides with a spectral resolution of 86,000 in the approximate wavelength range from $\lambda 380$ nm to $\lambda 875$ nm. Most of the spectra have a signal-to-noise ratio (SNR) between 60 and 140 in the V band, as shown in the third column of Table B3 and Fig. 3. Additionally, we took several spectra of the asteroid Vesta with the same spectrograph configuration. All the obtained spectra were reduced with the automatic pipeline for HERMES (Raskin et al. 2011). Next, we used several standard tasks within the IRAF environment for normalising the spectra, using a low-order polynomial fit to the observed continuum, and for applying the corresponding Doppler correction. To do so, we computed the observed radial velocity (V_r), which is the sum of the spectrum relative velocity (measured with the IRAF function `fxcor`) and barycentric correction (obtained from the FITS header). When several exposures were available for the same star, we combined all the individual spectra

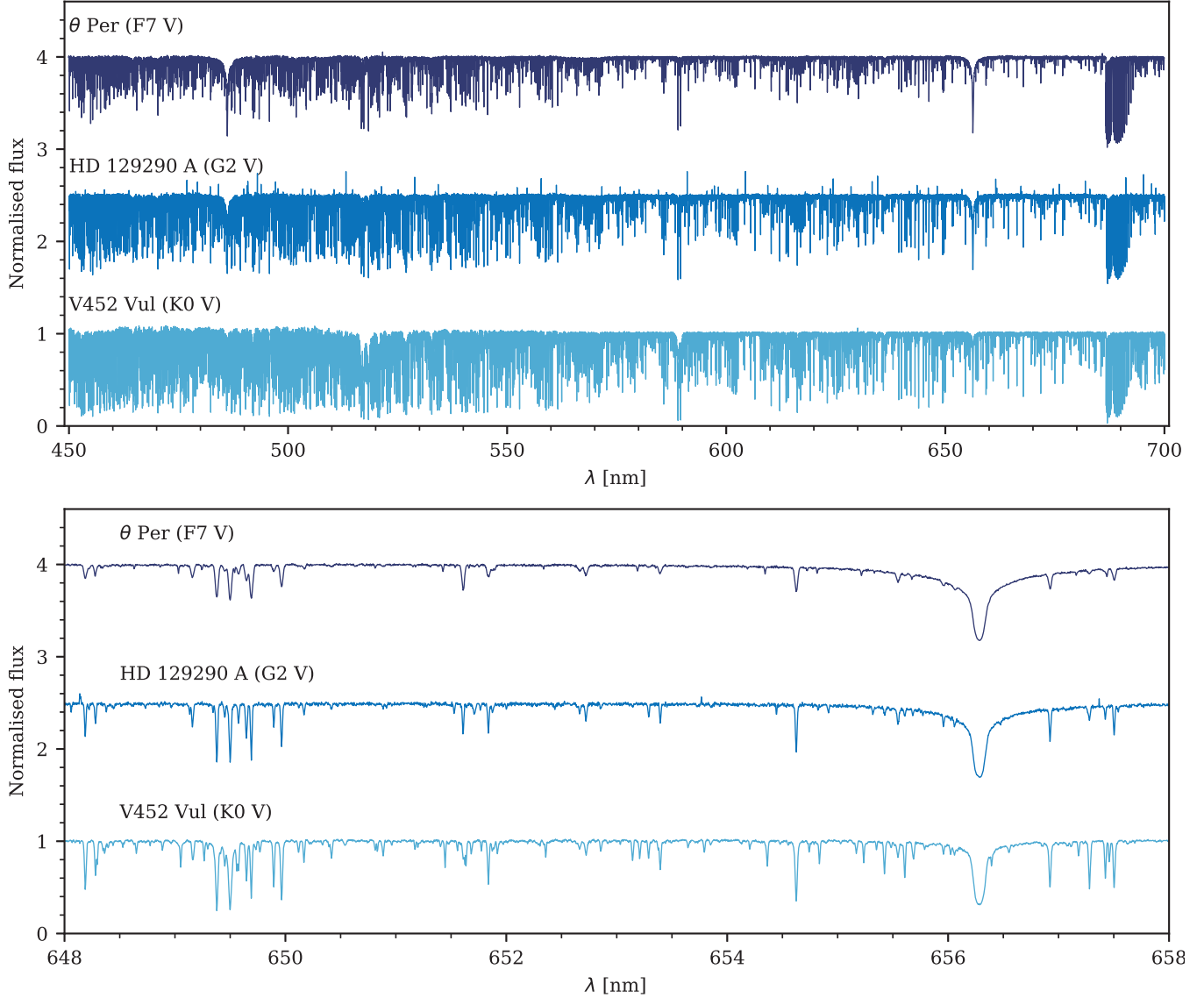


Figure 4. High-resolution spectra of three representative primaries (*from top to bottom*): θ Per, HD 129290 A, and V452 Vul (HD 189733). *Top:* Full investigated wavelength range. *Bottom:* zoomed range, 10 nm wide, near $H\alpha \lambda 656.3$ nm.

and obtained a unique spectrum with higher SNR. For our analysis we used only the wavelength range from 450 nm to 700 nm (Fig. 4). The 197 stars observed with HERMES are marked with ‘‘H’’ in the last column of Table B1.

We also observed many M-dwarf companions with the low-resolution optical spectrograph CAFOS at the 2.2 m Calar Alto telescope. They are marked with ‘‘C’’ (Alonso-Floriano et al. 2015a) and ‘‘C*’’ (unpublished) in the last column of Table B1. We are using these spectra for calibrating spectral indices and abundance determinations with features analysed at high spectral resolution, and will appear in forthcoming publications. In particular, seven of our M-dwarf companions (namely BX Cet, ρ^{02} Eri C, HD 233153, BD-02 2198, ρ^{01} Cnc B, θ Boo B, and HD 154363 B) have also been observed with the CARMENES spectrograph with very high SNR and spectral resolution (Quirrenbach et al. 2016; Reiners et al. 2018).

3.2 Stellar parameters

Stellar atmospheric parameters (effective temperature T_{eff} , surface gravity $\log g$, microturbulence velocity ξ , and iron abundance $[\text{Fe}/\text{H}]$, Section 4.2) were computed using the automatic STEPAR code (Tabernero, Montes & González Hernández 2012), which relies on the equivalent width (EW) method. We employed the 2014 version of the MOOG code (Sneden 1973) and a grid of Kurucz ATLAS9 plane-parallel model atmospheres (Kurucz 1993). As the damping prescription, we used the Unsöld approximation multiplied by a factor recommended by the Blackwell group (“option 2” within MOOG). We employed the line list of ~ 300 solar-calibrated Fe I and Fe II lines from Sousa et al. (2008). We measured their EW s using ARESv2 (Sousa et al. 2015). ARES input parameters

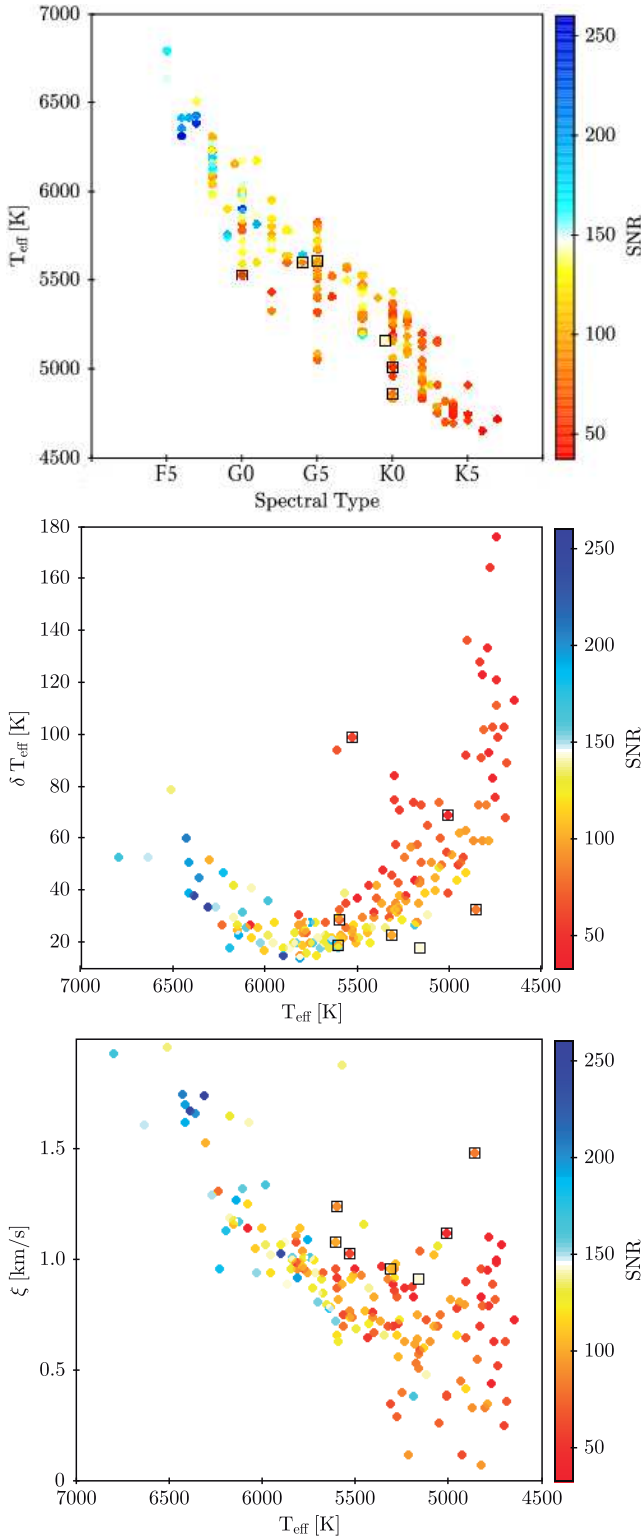


Figure 5. *Upper panel:* Effective temperature as a function of spectral type. *Middle panel:* Error in effective temperature as a function of the effective temperature. *Down panel:* Microturbulence velocity (ξ) against effective temperature. All the symbols are colour-coded with SNR. Black-ensquared stars represent low-gravity stars (Section 4.4).

Table 1. Solar parameters and element abundances.

Parameter	
T_{eff} [K]	5777±18
$\log g$	4.41±0.05
ξ [km s $^{-1}$]	0.91±0.03
Element	
$\log \epsilon (X)$	
Fe	7.48±0.01
Na	6.44±0.03
Mg	7.69±0.05
Al	6.51±0.01
Si	7.59±0.07
Ca	6.44±0.05
Sc	3.15±0.03
Ti	5.02±0.05
V	4.03±0.03
Cr	5.70±0.05
Mn	5.51±0.03
Co	4.95±0.03
Ni	6.30±0.07

were set to those recommended in its manual². The STEPAR code iterates within the parameter space until the slopes of χ vs. $\log \epsilon(\text{Fe i})$ and $\log EW\lambda$ vs. $\log \epsilon(\text{Fe i})$ are zero (i.e. the iron atoms are in excitation equilibrium). In addition, it imposes the ionisation equilibrium, such that $\log \epsilon(\text{Fe i})=\log \epsilon(\text{Fe ii})$. We also imposed that the [Fe/H] average of the MOOG output is equal to the iron abundance of the atmospheric model.

Table B3 shows the stellar atmospheric parameters of 198 F-, G-, and K- stars in our sample (193 primaries and 5 secondaries). The STEPAR code is based on an EW method that is meant to work for a limited range of T_{eff} . We were not able to determine with STEPAR the stellar atmospheric parameters of 21 stars:

- *Hot.* Stars with spectral types earlier than F6 ($T_{\text{eff}} \approx 6700$ K) do not have enough iron lines for our analysis. The triple system 9 Aur Aa,Ab,B comprises three stars of spectral types F2 V and early M, and the effective temperature reported in the literature is ~ 7000 K (Allende Prieto & Lambert 1999; Le Borgne et al. 2003). The star HD 27887 A, with an F5 V spectral type and $T_{\text{eff}} \approx 6500$ K (Allende Prieto & Lambert 1999; Katz et al. 2011) is at the boundary of our grid, and STEPAR did not converge either.

- *Cool.* Stars with spectral types later than K4 ($T_{\text{eff}} \approx 4500$ K), on the contrary to hot stars, have too many overlapping iron lines. We were not able to derive parameters for Aldebaran (K5 III, 3900 K; Soubiran et al. 1998; Prugniel et al. 2011) and SZ Crt (K7 V, 4200 K; Wright et al. 2011; Luck 2017).

- *Fast.* At high rotational velocities, iron lines become so broad that overlap, too. Six stars rotate too fast for STEPAR, i.e. have $v \sin i \gtrsim 10$ km s $^{-1}$. Published $v \sin i$ values for the six of them range from 16.2 km s $^{-1}$ for V368 Cep (Mishenina et al. 2012) to 84.8 km s $^{-1}$ for η UMi A (Schröder et al. 2009).

- *SB2.* We discarded double-line spectroscopic binaries with blended or partially blended lines. We found double peaks in spectral lines of eight primary stars; as discussed in Section 4.1, four are reported here for the first time. We were able to derive stellar atmospheric parameters for HD 200077 Aa1, the primary of a known

² <https://github.com/sousasag/ARES>, <http://www.astro.up.pt/~sousasag/ares/>

SB2 (see Section 4.1). There is a ninth SB2 in our sample, namely σ CrB Aa,Ab (Bakos 1984).

- *No obs.* We could not observe only one primary, the SB2 σ CrB Aa,Ab.

To sum up, we derived reliable spectroscopic stellar parameters for 175 primaries and 5 companions. Only σ CrB Aa,Ab (the “193rd” primary star) lacks our homogeneous spectroscopy. Stellar parameters derived with STEPAR are given in Table B3, together with [Fe/H] from the literature, when available. Fig. 5 shows the effective temperature and other parameters derived by us. In addition, as can be seen in the top part of Table 1, we have successfully derived the atmospheric parameters of the Sun (T_{eff} , $\log g$, ξ) by means of a solar spectrum (Vesta) taken with the HERMES spectrograph.

3.3 Abundances

In order to calculate the individual chemical abundances of the 180 stars, we assumed the stellar parameters derived with STEPAR. We obtained abundances for 13 different chemical species: Fe, the α -elements (Mg, Si, Ca, and Ti), the Fe-peak elements (Cr, Mn, Co, and Ni), and the odd-Z elements (Na, Al, Sc, and V). We calculated chemical abundances using the EW method, Kurucz ATLAS9 plane-parallel model atmospheres (Kurucz 1993), and the MOOG code (Sneden 1973), as in Tabernero et al. (2012, 2017). The EWs were determined using the ARES code (Sousa et al. 2015), following the approach described in Section 3.2. We also re-measured manually the EWs with the task splot within the IRAF environment when any individual abundance determination of particular lines was separated from the general trend. We computed final abundances in a differential manner (i.e., in a line-by-line basis) with respect to our solar spectrum (Vesta) observed with HERMES. See the resulting solar element abundances ($\log \epsilon(X)$) in the bottom part of Table 1. Table B4 reports these differential abundances ([X/H]) thus derived for our star sample.

3.4 Kinematics

Stellar kinematic groups (SKGs), superclusters (SCs), and moving groups (MGs) are kinematic coherent groups of stars that may share a common origin and, therefore, age and chemical composition (Boesgaard & Friel 1990; Eggen 1994; De Silva et al. 2007; Famaey et al. 2008; Antoja et al. 2009). Among them, the youngest SKGs are: the Hyades SC (~ 600 Myr), Ursa Major MG (Sirius SC ~ 400 Myr), Castor MG (~ 300 Myr), Local Association (Pleiades MG – 20 to 150 Myr), and IC 2391 SC (35–55 Myr). We refer the reader to Montes et al. (2001), López-Santiago et al. (2006), Klutsch et al. (2014), Riedel et al. (2017) and references therein for more details.

Other very young SKGs, such as the ϵ Chamaeleontis, TW Hydrae, β Pictoris, Tucana-Horologium, AB Doradus, Columba, Carina, and Hercules-Lyra moving groups, have kinematics close to the Local Association, as well as Argus’ to IC 2391, and Octans and Octans-Near’s to Castor (Zuckerman & Song 2004; Torres et al. 2008; Montes 2010, 2015; Bell et al. 2015). Even new associations are identified, such as the All Sky Young Association (ASYA – Torres et al. 2016).

With the coordinates in Table B1, parallactic distances and proper motions in Table B2, and radial velocities measured in Section 3.1, we computed Galactocentric space velocities as in Montes et al. (2001) with the procedure established

Table 2. Primary spectroscopic binaries.

WDS	Name	Type	Reference ^a
00452+0015	HD 4271 Aa,Ab	SB1	Gri01
00491+5749	Archid Aa,Ab	SB1	A&L76
02291+2252	BD+22 353Aa,Ab	SB1	Hal12
02482+2704	BC Ari Aa,Ab	SB1	Lat02
03206+0902	HD 20727 Aa,Ab	SB1	D&M91
03396+1823	V1082 Tau Aa,Ab	SB2	Lat92
03398+3329 ^b	HD 278874 Aa,Ab	SB2	This work
03566+5042	43 Per Aa,Ab	SB2	Wal73
05067+5136	9 Aur Aa,Ab	SB1	Abt65
05289+1233	HD 35956 Aa,Ab	SB1	Kat13
06173+0506 ^c	HD 43587	SB1	Kat13
09245+0621 ^b	HD 81212 AB	SB2	This work
09393+1319	HD 83509 Aa,Ab	SB2	Gri03
15282-0921 ^c	HD 137763	SB1	D&M92
16147+3352 ^d	σ CrB Aa,Ab	SB2	Bak84
16329+0315 ^c	HD 149162	SB1	Lat02
16348-0412	HD 149414 Aa,Ab	SB1	Lat02
20169+5017	HD 193216 Aa,Ab	SB1	Gri02
20462+3358	ϵ Cyg Aa,Ab	SB1	Gra15
20599+4016 ^c	HD 200077 Aa1,Aa2,Ab	SB2	Gol02
23026+2948 ^b	BD+29 4841Aa,Ab	SB2	This work
23581+2420 ^b	HD 224459 Aa,Ab	SB2	This work

^a Reference – Abt65: Abt (1965); A&L76: Abt & Levy (1976); Bak84: Bakos (1984); D&M91: Duquennoy & Mayor (1991); D&M92: Duquennoy et al. (1992); Gol02: Goldberg et al. (2002); Gra15: Gray (2015); Gri01: Griffin (2001); Gri02: Griffin (2002); Gri03: Griffin (2003); Hal12: Halbwachs et al. (2012); Kat13: Katoh et al. (2013); Lat92 Latham et al. (1992); Lat02: Latham et al. (2002); Wal73: Wallerstein (1973).

^b New SB2, discovered in this work.

^c Resolved close multiple system described in text.

^d Not observed by us.

by Johnson & Soderblom (1987). For the single- and double-lined spectroscopic binaries (Section 4.1) and the unobserved star σ CrB Aa,Ab, we adopted their systemic radial-velocity values γ from the literature. Table B5 lists the used radial velocities V_r along with the computed space velocities U , V , and W of our 198 F-, G-, and K-stars.

4 RESULTS AND DISCUSSION

We investigated 489 stars distributed in 193 systems, formed by 193 primary F-, G-, and K-stars and 296 common proper-motion companions and candidates (Table B1). For these systems, we studied their proper motions and distances, as explained in Section 2. We got a final sample of 192 physical systems, of which 135 are double and 57 are multiple (43 triple, 9 quadruple, and 5 quintuple). In Table B2 we marked the 84 discarded stars, along with other useful remarks for the remaining stars.

4.1 Spectroscopic binaries

As discussed in Section 3.2, we were not able to determine stellar parameters for seven double-peak spectroscopic binaries (SB2s). They are listed in Table 2, together with the other SB2s σ CrB Aa,Ab (not observed) and HD 200077 Aa,Ab (with stellar parameters). We report for the first time four SB2s, namely HD 278874 Aa,Ab, HD 81212 AB, BD+29 4841 Aa,Ab, and

HD 224459 Aa,Ab. Only for the later, we have two HERMES spectra separated by one day but we could not see any significant difference between them, so the orbital period must be $P_{\text{orb}} \gg 1$ d. Interestingly, HD 81212 AB was found to be an astrometric binary by F. G. W. Struve in 1831. The pair is separated by $\rho = 1.1\text{--}1.9$ arcsec and, thus, unresolved by us. The very small magnitude difference between A and B, $\Delta m \approx 0.12$ mag, indicates a mass ratio close to unity. We estimate an orbital period of 200–300 yr for the astrometric pair, and a radial-velocity difference of about 6 km s^{-1} , which is consistent with what we observe in the double-line spectroscopic binary. Therefore, the spectroscopic binary can actually be the astrometric binary. This fact could also explain the apparently wrong parallax tabulated by TGAS. The other three new SB2 stars are not known close astrometric binaries.

There are full orbital parameters (P , e , γ , K_1 , K_2) available in the literature for the other five stars, including σ CrB Aa,Ab and HD 200077 (S_{B9} – Pourbaix et al. 2004). The latter is part of a quintuple system containing a close SB2 (F8 V + G6–9; $P = 112.5$ d) first resolved by Horch et al. 2012 (LSC 1, $\rho \approx 0.022$ arcsec), a close companion resolved by *Hipparcos* (late K; COU 2431, $\rho = 2.2$ arcsec), and the wide cool companion G 210–44 (K7 V + M0–1;), which is in turn another close binary (Latham et al. 1988; Goldberg et al. 2002; Mazeh et al. 2003; Caballero 2009). In our HERMES spectra of HD 200077, the Aa1 component (late F) dominates over Aa2 (late G) and Ab (late K, not visible), and its lines were well separated from those of the other components.

Besides, there are 13 known single-line spectroscopic binaries (SB1) in our sample. We did not discard them in our analysis because the determined stellar parameters correspond to the primary in the system and were not significantly affected by the companion. Four of the SB1s were also resolved astrometrically:

- HD 43587 (CAT 1, $\rho \approx 0.90$ arcsec). The orbital period of $P = 34.2$ yr determined by Katoh et al. (2013) from radial-velocity monitorisation matches reasonably well the adaptive optics observations by Catalá et al. (2006). The system deserves a new analysis given the low mass of the companion, several magnitudes fainter than the primary.
- HD 137763 (BAG 25, $\rho \approx 0.10$ arcsec). The orbital period of $P = 2.44$ yr determined by Duquennoy et al. (1992) also matches the measured projected physical separations measured astrometrically (Jancart et al. 2005; Balega et al. 2006; Horch et al. 2015), and, therefore, the dynamical masses of the two stars can be determined precisely.
- HD 149162 (DSG 7, $\rho \approx 0.0148$ arcsec and $\rho \approx 0.284$ arcsec). Again, the astrometric measurements of Horch et al. (2015) agree with the spectroscopic measurements of Latham et al. (2002), who determined an orbital period of 0.620 yr. This is a hierarchical triple system, and the seven-month period of the SB1 corresponds to the closest pair. The effect of the component at ~ 0.3 arcsec is not discernible spectroscopically. The wide common proper motion companion, at 4.2 arcmin to the south east, is in turn a binary made of an M3.0 V star and a white dwarf, which makes HD 149162 a quintuple system.
- ϵ Cyg (CHR 100, $\rho = 0.041$ arcsec). This well-studied, binary giant star has been the subject of numerous radial-velocity surveys (e.g. Griffin 1994; Gray 2015) and has also been resolved with optical interferometry (Hartkopf et al. 1994).

4.2 [Fe/H]

We derived stellar atmospheric parameters of 175 primaries and five secondaries (Section 3.2 and Table B3), from which 50 are presented here for the first time. One of the parameters is the iron abundance [Fe/H], which is the most used proxy for metallicity. In the left panel of Fig. 6, we depict spectroscopic [Fe/H] collected from the literature against the ones derived by us. For a fair comparison, we only collected spectroscopic [Fe/H] from the literature (e.g., Valenti & Fischer 2005; Sousa et al. 2011; Ramírez et al. 2013; Santos et al. 2013), and did not take into account the ones derived photometrically (e.g., Bonfils et al. 2005; Johnson & Apps 2009; Schlaufman & Laughlin 2010). We compiled and selected spectroscopic [Fe/H] with the PASTEL Catalogue (Soubiran et al. 2016), giving priority to the most recent works. According to the diagram, our values agree very well with the published ones, mainly in the range of $-1.0 < [\text{Fe}/\text{H}] < 0.5$ and no significant offset is detected. The iron abundance determined by us does not display any trend as a function of T_{eff} or $\log g$, as shown in the right panel of Fig. 6,

The least metallic star in our sample is the red giant branch star BD+80 245 (G0 IV). We measured $[\text{Fe}/\text{H}] = -1.58 \pm 0.07$, a value slightly higher than those provided by Fulbright (2000, $[\text{Fe}/\text{H}] = -2.05$), Stephens & Boesgaard (2002, $[\text{Fe}/\text{H}] = -1.76$), and Roederer et al. (2014, $[\text{Fe}/\text{H}] = -2.04$). BD+80 245 was also studied by Ivans et al. (2003), who classified it as a halo star based on its chemical composition (we also classified it as a halo star in Section 4.5 based on kinematics), and explained a possible formation from material polluted by the earliest supernovae Ia events that occurred in the Milky Way. BD+80 245 is the only star that stays away from the general trend in the left panel of Fig. 6.

In general, [Fe/H] has an effect on the derivation of spectro-photometric distances (Section 2). As illustrated in Fig. 2, stars with $[\text{Fe}/\text{H}] < -0.4$ tend to lie in the upper part of the 1:1 relation between primary and “secondary” distances. This effect may be due to an intrinsic offset in the spectral type– M_J relation used to derive spectro-photometric distances to our late-K and M dwarfs, as Cortés-Contreras et al. (2017) assumed solar metallicity (all 192 physical primaries have parallactic distances but 160 companions have spectro-photometric distances). The two low-metallicity systems that suffer more from this offset are WDS 03150+0101 (BD+00 549A, with $[\text{Fe}/\text{H}] = -0.88$, and BD+00 549B), and WDS 22090-1754 (HD 210190, with $[\text{Fe}/\text{H}] = -0.42$, and LP 819-37, with $\zeta = 0.856$, where ζ is a metallicity spectral index defined by Lépine et al. 2007 and measured by Alonso-Floriano et al. 2015a). For these systems, the spectro-photometric distances for the secondary component are about twice as large as the parallactic distance of the primary.

Besides, for WDS 16348-0412 (HD 149414 Aa,Ab, with $[\text{Fe}/\text{H}] = -1.16$, and GJ 629.2B, with $\zeta = 0.664$) we did not derive a spectro-photometric distance for the secondary because it is a sub-dwarf candidate (sdM0; Alonso-Floriano et al. 2015a)³. Instead, we adopted the spectro-photometric distance of 48^{+12}_{-9} pc from the M_J -SpT relationship for subdwarfs in Zhang et al. (2013), which agrees with the distance to its very low metallicity primary tabulated by TGAS of 46.3 ± 0.9 pc. We concluded that the metallicity affects the derivation of our spectro-photometric distances, but heterogeneously and in extreme cases.

³ Note the wrong spectral type of GJ 629.2B in Simbad.

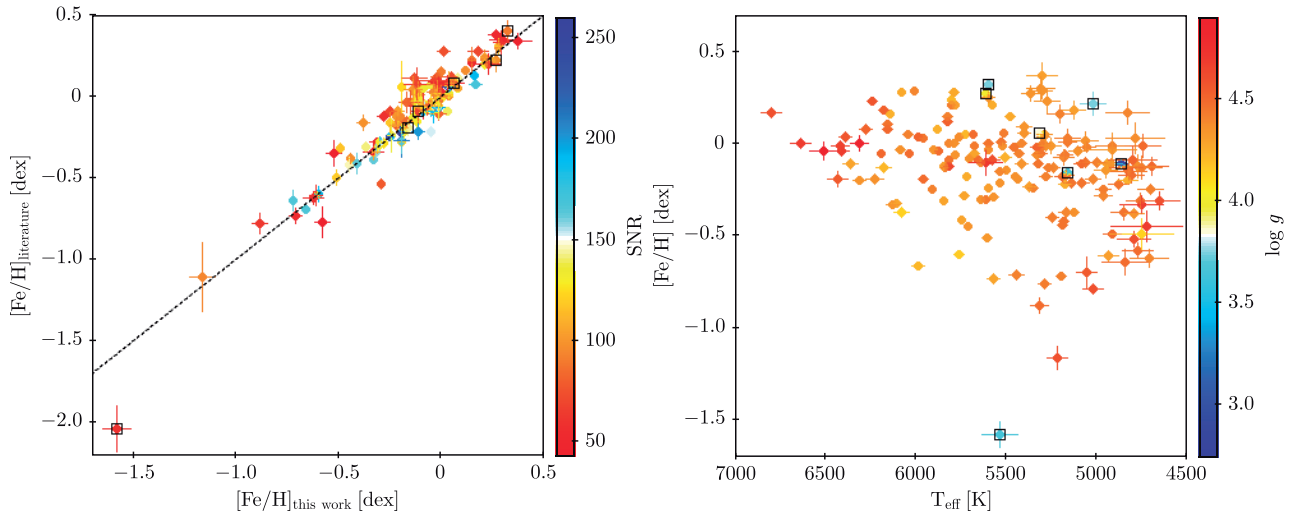


Figure 6. Left panel: iron abundance published in the literature against that obtained in this work, colour-coded with SNR. Black dashed line represents 1:1 relation. Right panel: iron abundance as a function of effective temperature for our primary stars, colour-coded with $\log g$. Black-ensquared stars represent low-gravity stars.

Table 3. Estimated ages for the seven low-gravity stars ($\log g < 4.1$) with stellar parameters in our sample.

WDS	Simbad	$\log g$	[Fe/H]	Estimated age [Gyr]	Published age [Gyr]	Reference ^a
01572-1015	HD 11964 A	3.85±0.06	0.06±0.02	~5–10	9.77±0.52	Tsa13
05466+0110	HD 38529 A	3.75±0.07	0.32±0.02	~2–5	3.77±0.36	Ram12
08110+7955	BD+80 245	3.63±0.20	-1.58±0.07	~13–14
11523+0957	HD 103112	3.75±0.19	0.22±0.06	~10
17465+2743	μ^01 Her A	4.03±0.04	0.27±0.02	~10	7.88±0.24	Ram12
19553+0624	β Aql A	3.64±0.06	-0.16±0.01	~2–5	4.08±3.95	Ram13
20462+3358	ϵ Cyg A	2.74±0.11	-0.11±0.03	~1	0.90±0.20	daS15

^aReference – Ram12: [Ramírez et al. \(2012\)](#); Ram13: [Ramírez et al. \(2013\)](#); Tsa13: [Tsantaki et al. \(2013\)](#); daS15: [da Silva et al. \(2015\)](#).

4.3 Abundances

Apart from iron, we measured chemical abundances of 12 different elements for the 180 F-, G-, and K- stars in our sample (Na, Mg, Al, Si, Ca, Sc, Ti, V, Cr, Mn, Co, and Ni – see Section 3.3 and Table B4). Galactic trends are depicted in Figs. A1 and A2 where we plot the abundance ratios of [X/Fe] versus [Fe/H] for each element X. We compared them to the FGK stellar sample from Adibekyan et al. (2012). Our sample covers a wide range of [Fe/H] and includes a few low-metallicity stars ([Fe/H] < -1.0) that fall well below the range studied by Adibekyan et al. (2012) and, as expected, have enhanced content in α elements (Bensby et al. 2014; Jofré et al. 2015).

Using our line-by-line differential analysis we reproduced the expected behaviour of the different chemical species, with manganese being a remarkable exception. Useful Mn lines are scarce and difficult to measure in our HERMES spectra either by hand (with IRAF splot) or with a semiautomatic method (using the ARES code), and thus our results present an offset that reflects this fact. Interestingly, we also reproduced the scatter found by Adibekyan et al. (2012) for vanadium and scandium, which is a known issue for stars cooler than 5000 K (see Neves et al. 2009 and Tabernero et al. 2012 for further details). Giants and subgiants tend to deviate from the general trends. Although this effect appears to

be entirely real (Smiljanic 2012; Tabernero et al. 2012), it is not observed in these cases, and, therefore, may be an effect only on very low gravity stars ($\log g \leq 2.5$).

4.4 Giants and subgiants

Among our list of 192 physical primaries there are eight stars with surface gravities lower than $\log g = 4.1$ (see Fig. 7). They are Aldebaran ($\log g = 1.66$; Prugniel et al. 2011), for which we were not able to determine stellar parameters with STEPAR, the giant star ϵ Cyg A ($\log g = 2.74$), BD+80 245 ($\log g = 3.63$), which is the red giant branch star with the lowest metallicity in our sample, and five subgiant stars with $\log g = 3.64$ –4.03. Of them, HD 103112 had not been reported before to display any subgiant class or low-gravity feature in its spectra (but see McDonald et al. 2017 and their photometric analysis). The remaining four subgiants are quite well investigated, either because of their brightness (β Aql A and μ^01 Her A) or presence of exoplanets (HD 11964 A and HD 38529 A; Section 4.6).

For the seven low-gravity stars with derived stellar parameters, we estimated their ages using the Yale-Potsdam Stellar Isochrones (YaPSI – Spada et al. 2017) with two different iron abundances ([Fe/H] = 0.0 and [Fe/H] = -1.5) and fixed solar helium abundance ($Y = 0.28$; see again Fig. 7). Estimated ages agree within uncer-

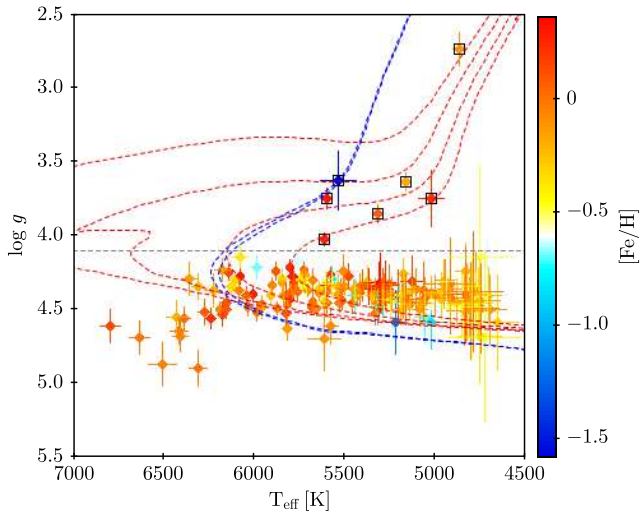


Figure 7. Surface gravity as a function of effective temperature for our primary stars, colour-coded with metallicity. Red dashed lines correspond to isochrones of $[Fe/H] = 0.0$ and ages of 1, 2, 5, and 10 Gyr, from top to bottom. Blue dashed lines correspond to isochrones of $[Fe/H] = -1.5$ and ages of 13 and 14 Gyr. All isochrones are from YaPSI (Spada et al. 2017). The grey, horizontal, dashed line correspond to $\log g = 4.1$.

tainties with published values in five cases (Table 3). We determined ages for the first time for the two remaining stars: the poorly-investigated subgiant HD 103112 and the very low-metallicity star BD+80 245. For the later, we infer an age similar to that of the Universe (limited by the accuracy of the YaPSI models), which is consistent with the hypothesis of Evans et al. (2003) of it being a halo star polluted by the earliest supernova explosions.

4.5 Kinematics

As illustrated by the Toomre diagram (Fig. 8), we classified each star in the different Galactic populations, halo (H), thick disc (TD), thick-to-thin transition disc (TD-D), and thin disc (D), as in Bensby et al. (2003, 2005). For that, we assumed Gaussian distributions of space velocities U , V , and W . We found 165 stars in the thin disc, 23 in the thick disc, 7 in the thick-to-thin transition disc, and 3 in the halo, as it is shown in Table B5 and Fig. 8. The three stars in the halo are:

- Ross 413. It is a halo star catalogued by Allen & Monroy-Rodríguez (2014) in the context of MACHO studies. The iron abundance derived by us, $[Fe/H] = -0.58$, is again slightly higher than the published value ($[Fe/H] = -0.77$; Woolf & Wallerstein 2005).
- BD+80 245. It is the old, low-metallicity, subgiant star discussed above. Our classification as an halo star agrees with the one published in Evans et al. (2003; see Section 4.2).
- HD 149414. It is a well-studied halo star (e.g. Sandage 1969; Tomkin & Lambert 1999; Gratton et al. 2003; Allen & Monroy-Rodríguez 2014), and the star with the second lowest iron abundance in our sample ($[Fe/H] = -1.16$). Besides, it is also a single-lined spectroscopic binary (Table 4.1).

In general, thick-disc (and also thick-to-thin-transition-disc) stars have subsolar metallicities. However, there are some remarkable outliers, such as HD 102326 ($[Fe/H] = +0.15 \pm 0.02$), HD 103112 ($[Fe/H] = +0.22 \pm 0.06$), and HD 190360 ($[Fe/H] =$

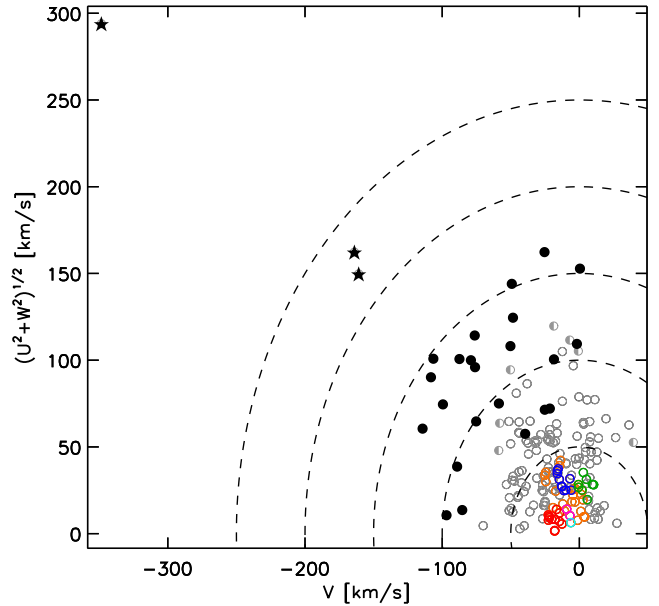


Figure 8. Toomre diagram of our F-, G-, and K- stars. Black stars: halo; black filled circles: thick disc; grey semi-filled circles: thick-to-thin transition disc; grey open circles: thin disc. Blue: Hyades SC; red: Local Association; green: Ursa Major MG; magenta: IC 2391 SC; cyan: Castor MG; orange: other young stars. Dashed grey lines represent constant values of the total space velocity $v_{tot} = (U^2 + V^2 + W^2)^{1/2}$ in steps of 50 km s^{-1} . The Galactocentric space velocities U , V , and W are referred to the local standard of rest.

$+0.21 \pm 0.02$), which may represent the tail of the distribution towards high metallicities or, conversely, a kinematic classification at the boundary with the thin disc.

Next, for the stars in the thin disc, we separated between young disc stars and non-young disc stars (designated with the symbol 'x' in Table B5) as defined by Eggen (1984, 1989) and depicted in the Böttlinger diagram (Fig 9). Thick disc, thick-to-thin transition disc, and halo stars are also non-young disc stars. Besides, for each young disc star, we studied its membership in known SKGs, also as in Montes et al. (2001). In particular, we identified 33 star candidates in SKGs: 12 stars in the Local Association, 10 in the Hyades SC, eight in the Ursa Major MG, two in the IC 2391 SC, and one in the Castor MG, whereas 20 are young disc star with no apparent SKG membership (designated with 'YD' in Table B5). Also, we checked the membership of our 33 young Galactic disc stars with the LACEWING (Riedel et al. 2017) and BANYAN Σ (Gagné et al. 2018)⁴ algorithms. As summarised in Table B5, of the 33 stars candidates in known SKGs, 17 had been already proposed to belong to some of them.

• Local Association. Seven of our 12 LA candidates were already classified as probable LA members by Montes et al. (2001). All of them except HD 98736 had been later assigned to SKGs linked to the LA, which supports our classification: Hercules-Lyra (V538 Aur and V382 Ser, by Fuhrmann 2004; DX Leo and HH Leo, by Eisenbeiss et al. 2013), AB Doradus (V577 Per, by Riedel et al. 2017), and Columba (V368 Cep, with BANYAN Σ). The eighth known LA star candidate is HD 82939, which proper-motion companion MCC 549 has been subject of debate: Schlieder et al. (2012) proposed it to be a member in the β Pictoris

⁴ <http://www.exoplanetes.umontreal.ca/banyan/banyansigma.php>

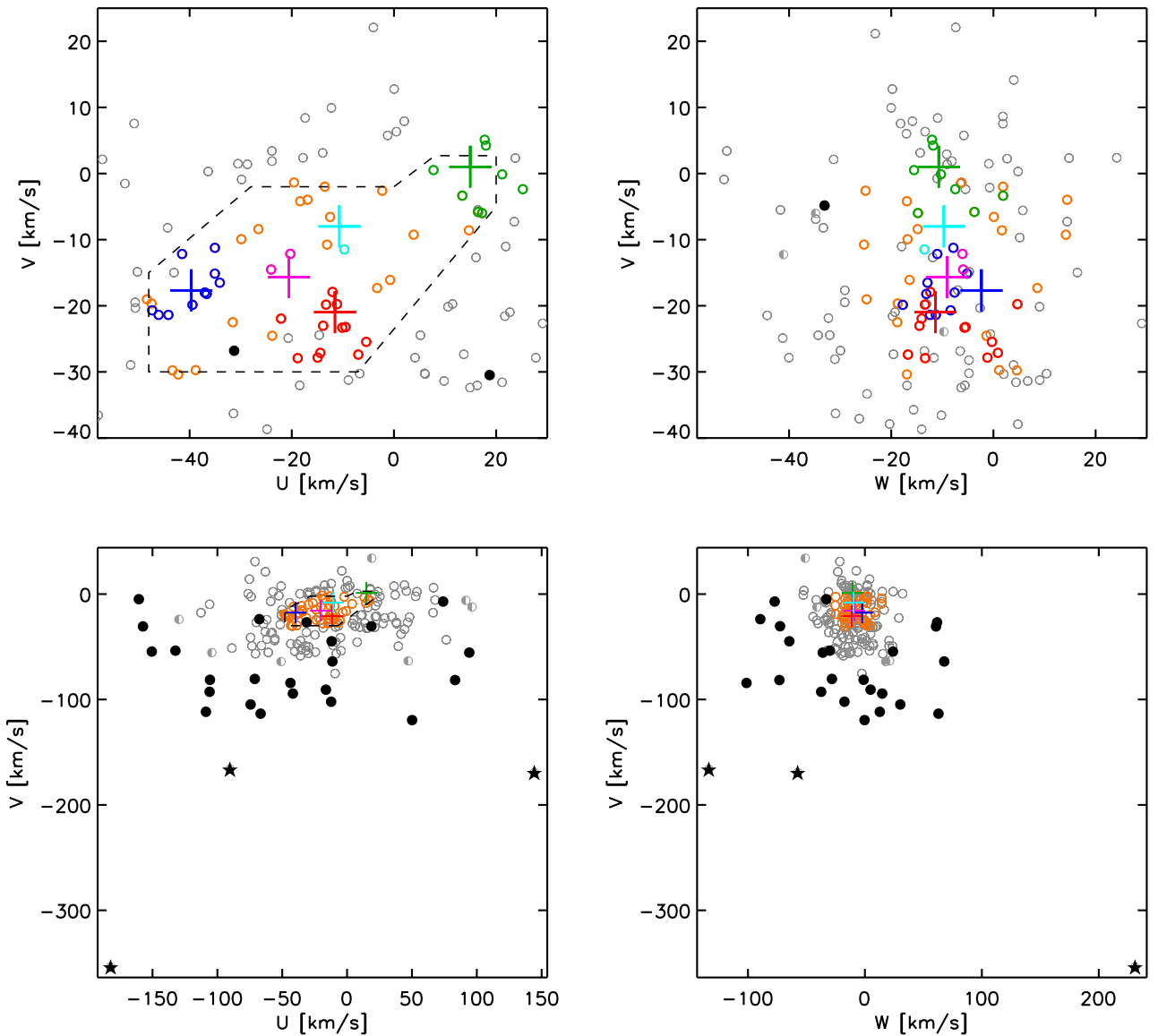


Figure 9. Same as Fig 8, but for the Böttlinger diagrams. Crosses mark the centres of each young SKG. Upper panels represent zoomed areas of lower panels. In the top left panel, the dashed grey line confines the young disc population as defined by Eggen (1984, 1989).

moving group, also linked to the LA, but this statement was later denied by Malo et al. (2014) and Shkolnik et al. (2017). There is no trail of lithium in our HERMES spectrum of HD 82939 (G5 V), which supports the Malo et al. (2014) conclusion.

- Hyades super-cluster. We recovered two stars previously considered as members of the Hyades SC using different methods: the multi-planet host ρ^01 Cnc A (aka Copernicus, 55 Cnc), with chemical tagging (Tabernero et al. 2012), and HD 51067 A, with LACEwING (Riedel et al. 2017). Besides, HD 116963 could be a Carina-Near star according to BANYAN Σ .

- Ursa Major moving group. Four stars were confirmed as UMa MG members by chemical tagging in Tabernero et al. (2017): the pair WDS J05445-2227 (γ Lep and AK Lep), V869 Mon, and HD 167389. Another two stars, HD 24961 and SZ Crt, were also classified as UMa MG members by Montes et al. (2001), King et al. (2003), and López-Santiago et al. (2010).

- IC 2391 super-cluster. V447 Lac was classified as a doubtful member in Hercules-Lyra by Eisenbeiss et al. (2013), but a more

recent analysis by Riedel et al. (2017) located it in the Argus moving group, which is kinematically linked to the IC 2391 super-cluster.

We computed the mean iron abundance for each SKG and compared them with the ones published in the literature (Boesgaard & Friel 1990; Randich et al. 2001; Paulson et al. 2003; Vauclair et al. 2008; Pompéia et al. 2011; Tabernero et al. 2012; De Silva et al. 2013; Tabernero et al. 2017), and found a good agreement between them. Although this is not an exhaustive chemical tagging analysis, it supports our kinematic classification.

4.6 Planetary systems with late-type dwarfs

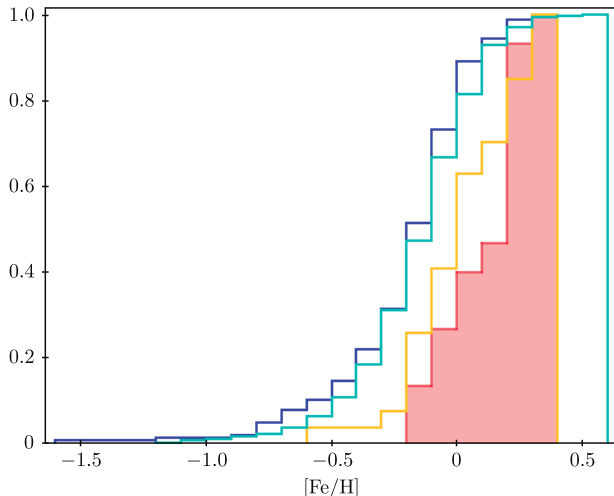
As González (1997), Santos et al. (2001) and Fischer & Valenti (2005) reported for the first time, the probability of hosting a giant exoplanet tends to increase with the iron abundance (metallicity) of F-, G-, and K- dwarf stars. This relationship has

Table 4. F, G, K- stars with confirmed exoplanets in our sample.

WDS	Primary	[Fe/H]	Planet(s)	Reference ^a	Secondary	s [au]
01572-1015	HD 11964 A	0.06±0.02	b, c	Wri09	HD 11964 B	974±23
03480+4032	HD 23596	0.28±0.02	b	Per03	J03480588+4032226	3693±52
04359+1631	Aldebaran	-0.27±0.05 ^b	b	Hat15	Aldebaran B	573±11
05466+0100	HD 38529 A	0.32±0.02	b, c	Ben10	HD 38529 B	11148±175
06332+0528	HD 46375 A	0.23±0.06	b	WF11	HD 46375 B	363±12
08526+2820	ρ^01 Cnc A	0.29±0.04	b, c, d, e, f	Nel14	ρ^01 Cnc B	1044±10
09152+2323	HD 79498	0.21±0.02	b	Rob12	BD+23 2063B	2768±80
13018+6337	HD 11337 A	0.17±0.03	b	Bor14	LSPM J1301+6337	4419±48
18006+2943	HD 164595 A	-0.08±0.01	b	Cou15	HD 164595 B	2509±27
18292+1142	HD 170469	0.28±0.02	b	Fis07	J18291369+1141271	2617±37
20007+2243	V452 Vul	-0.10±0.03	b	Sou10	J20004297+2242342	224±2
20036+2954	HD 190360 A	0.21±0.02	b, c	Vog05	HD 190360 B	2854±27
21324-2058	HD 204941	-0.19±0.03	b	Dum11	LP 873-74	1610±12
23419-0559	HD 222582 A	0.00±0.02	b	But06	HD 222582 B	4637±59

^a Reference – Ben10: Benedict et al. (2010); Bor14: Borgniet et al. (2014); But06: Butler et al. (2006); Cou15: Courcol et al. (2015); Dum11: Dumusque et al. (2011); Fis07: Fischer et al. (2007); Hat15: Hatzes et al. (2015); Nel14: Nelson et al. (2014); Per03: Perrier et al. (2003); Rob12: Robertson et al. (2012); Sou10: Southworth (2010); Vog05: Vogt et al. (2005); WF11: Wang & Ford (2011); Wri09: Wright et al. (2009).

^b: Iron abundance from Hatzes et al. (2015).

**Figure 10.** Normalised cumulative iron abundance histogram of the stars in our sample with (red, shaded) and without planets (blue), and of the Sousa et al. (2011) sample with (yellow) and without planets (cyan).

been investigated and confirmed in detail afterwards by many other authors (González 2006; Guillot et al. 2006; Pasquini et al. 2007; Ghezzi et al. 2010; Johnson et al. 2010; Sousa et al. 2011; Buchhave et al. 2018). However, this relationship has not been found to hold for M dwarfs (Laughlin et al. 2004; Johnson & Apps 2009; Hobson et al. 2018).

We searched for confirmed exoplanet discoveries around our 193 primaries using The Extrasolar Planet Encyclopaedia⁵. The identified planetary systems are listed in Table 4, along with our derived iron abundance and the projected physical separation s between primary and companion. The separations between stars in a system is much larger than between star and planet (e.g. ~ 7000

times in the case of V452 Vul, also known as HD 189733; Martin 2018).

We found that 14 of our FGK primaries have, at least, one confirmed exoplanet. Of them, ten have a derived iron abundance $[Fe/H] \geq 0.0$, and of these ten, eight have $[Fe/H] \geq 0.15$, including the five-planet host ρ^01 Cnc A. This new proof of the planet-metallicity relation is illustrated by Fig. 10. As depicted, the detection probability of exoplanets in both Sousa et al. (2011) sample and ours tends to be higher when the iron abundance increases.

We performed a Kolmogorov-Smirnov test to assess the difference between the stars with and without planets in our sample. At the 2σ level, we can safely say that they are significantly different. We also repeated the test for the Sousa et al. (2011) sample and found the same result at the same confidence level. In addition, we compared our subsamples with Sousa et al. (2011)'s and found no difference between them (with and without planets) at the 2σ level confidence, in spite of the iron abundance range of stars with exoplanets in the Sousa et al. (2011) sample ($-0.50 \leq [Fe/H] \leq +0.40$) being slightly wider than ours ($-0.20 \leq [Fe/H] \leq +0.40$).

In order to prove the planet-metallicity relation in M dwarfs, we have prepared Table 5. It tabulates the 13 most metallic ($[Fe/H] \geq 0.16$), late-K- and M-dwarf companions of our sample brighter than $J = 10.5$ mag and without companion at $\rho < 5$ arcsec (exactly as in the CARMENES radial-velocity survey – Caballero et al. 2016). They should be high-priority targets of exoplanet searches, as they have the same iron abundance as their primaries if they were born in the same molecular cloud. Six late-type dwarfs in Table 5 are already common proper-motion companions to FGK-type stars with known exoplanets (Table 4). Interestingly, of the 13 M dwarfs, only one is being monitored in radial velocity by CARMENES, which sample is unbiased by metallicity or activity (Reiners et al. 2018).

5 CONCLUSIONS

This is the first item of a series of papers devoted to improve the metallicity calibration and to investigate the abundances of M

⁵ <http://exoplanet.eu/>

Table 5. Single late-K and M dwarf companions with $[\text{Fe}/\text{H}] > 0.16$.

WDS	Late-type companion	SpType	$[\text{Fe}/\text{H}]$
02556+2652	HD 18143 B	K7 V	0.18±0.05
	HD 18143 C	M4.0 V	0.18±0.05
03480+4032 ^a	J03480588+4032226	M1.5 V	0.28±0.02
04429+1843	HD 285970	K5 V	0.24±0.02
05466+0100 ^a	HD 38529 B	M2.5 V	0.32±0.02
06332+0528 ^a	HD 46375 B	M2.0 V	0.23±0.06
07191+6644	HD 55745 B	M0.0 V	0.23±0.02
08526+2820 ^{a,b}	ρ^{01} Cnc B	M4.5 V	0.29±0.04
09152+2323 ^a	BD+23 2063B	M0.0 V	0.21±0.02
10010+3155	20 LMi B	M6.0 V	0.21±0.01
11218+1811	HD 98736	M0.0 V	0.30±0.06
20036+2954 ^a	HD 190360 B	M4.5 V	0.21±0.02
23104+4901	HD 218790	K5 V	0.29±0.01

^a: FGK-type primary with confirmed exoplanet. See Table 4.

^b: M dwarf being monitored by CARMENES.

dwarfs. For that, we investigate wide binary and multiple benchmark systems containing solar-like primaries and M-dwarf companions. Here we present the sample and our first results on physical companionship, stellar parameters, abundances, and kinematics of the primaries.

Here we characterised a sample of 489 stars distributed in 193 binary and multiple candidate systems formed by a late-F-, G-, or early-K primaries and at least late-K- or M-dwarf companion candidate. For each of them, we compiled or derived coordinates, spectral types, J -band magnitudes, proper motions, and heliocentric distances. After a common proper-motion analysis, we ended up with a sample of 192 binary and multiple physical FGK+M systems. With HERMES at the 1.2 m Mercator Telescope, we obtained high-resolution optical spectra of 197 stars and, after excluding spectroscopic binaries, fast rotators, and hot and cool stars, we derived stellar atmospheric parameters for 175 primaries and five companions with the the STEPAR code. We measured effective temperature T_{eff} , surface gravity $\log g$, microturbulence velocity ξ , and photospheric chemical abundances for 13 atomic species, including iron. For 50 stars we tabulated the first measure of $[\text{Fe}/\text{H}]$. We estimated ages for the seven stars with the lowest surface gravity using isochrones for different iron abundances. We computed Galactocentric space velocities U , V , and W for the 198 FGK stars, and compared them with the ones published in the literature. We identified three systems in the Galactic halo, 23 systems in the thick disc, and 33 systems in young stellar kinematic groups (of which 16 are new candidates). Finally, we studied the presence of exoplanets around our F-, G- and K-type primaries, and provided a list of late-type dwarf companions useful to test the planet-metallicity relation in M dwarfs under the assumption that companions have the same metallicity as primary stars.

Forthcoming papers of this series will focus on the calibration of spectral indices from optical to infrared low-resolution spectra and photometry of M-dwarf companions with the metallicity of their primaries. We will also derive stellar atmospheric parameters and abundances of the M-dwarf companions with spectral synthesis on high-resolution spectra, and compare the results with the values presented here, which will be very useful for other groups worldwide.

ACKNOWLEDGEMENTS

This research made use of the SIMBAD database and VizieR catalogue access tool, operated at Centre de Données astronomiques de Strasbourg, France, the Spanish Virtual Observatory, the NASA’s Astrophysics Data System, and the Washington Double Star Catalog maintained at the U.S. Naval Observatory. Financial support was provided by the Universidad Complutense de Madrid, the Comunidad Autónoma de Madrid, the Spanish Ministerio de Economía y Competitividad (MINECO) and the Fondo Europeo de Desarrollo Regional (FEDER/ERF) under grants AYA2016-79425-C3-1/2-P, AYA2015-68012-C2-2-P, AYA2014-56359-P, RYC-2013-14875, and FJCI-2014-23001, the Conserjería de Educación, Juventud y Deporte de la Comunidad de Madrid, and the Fondo Social Europeo y la Iniciativa de Empleo Juvenil (YEI) under grant PEJD-2016/TIC-2347, and the Spanish Ministerio de Educación, Cultura y Deporte, programa de Formación de Profesorado Universitario under fellowship FPU15/01476. Finally, we would like to thank the anonymous referee for helpful comments and corrections.

REFERENCES

- Abt H. A., 1965, [ApJS](#), **11**, 429
- Abt H. A., Levy S. G., 1976, [ApJS](#), **30**, 273
- Adibekyan V. Z., Sousa S. G., Santos N. C., Delgado Mena E., González Hernández J. I., Israelian G., Mayor M., Khachatryan G., 2012, [A&A](#), **545**, A32
- Allen C., Monroy-Rodríguez M. A., 2014, [ApJ](#), **790**, 158
- Allende Prieto C., Lambert D. L., 1999, [A&A](#), **352**, 555
- Alonso-Floriano F. J., et al., 2015a, [A&A](#), **577**, A128
- Alonso-Floriano F. J., Caballero J. A., Cortés-Contreras M., Solano E., Montes D., 2015b, [A&A](#), **583**, A85
- Altmann M., Roeser S., Demleitner M., Bastian U., Schilbach E., 2017, [A&A](#), **600**, L4
- Ammler-von Eiff M., Bedalov A., Kranhold C., Mugrauer M., Schmidt T. O. B., Neuhäuser R., Errmann R., 2016, [A&A](#), **591**, A84
- Andrews J. J., Chanamé J., Agüeros M. A., 2018, [MNRAS](#), **473**, 5393
- Antoja T., Valenzuela O., Pichardo B., Moreno E., Figueras F., Fernández D., 2009, [ApJ](#), **700**, L78
- Bakos J. A., 1984, [AJ](#), **89**, 1740
- Balega I. I., Balega A. F., Maksimov E. V., Malogolovets E. A., Pluzhnik E. A., Shkhagosheva Z. U., 2006, Bulletin of the Special Astrophysics Observatory, **59**, 20
- Baraffe I., Chabrier G., Allard F., Hauschildt P. H., 1998, [A&A](#), **337**, 403
- Bean J. L., Sneden C., Hauschildt P. H., Johns-Krull C. M., Benedict G. F., 2006a, [ApJ](#), **652**, 1604
- Bean J. L., Benedict G. F., Endl M., 2006b, [ApJ](#), **653**, L65
- Bell C. P. M., Mamajek E. E., Naylor T., 2015, [MNRAS](#), **454**, 593
- Benedict G. F., McArthur B. E., Bean J. L., Barnes R., Harrison T. E., Hatzes A., Martioli E., Nelan E. P., 2010, [AJ](#), **139**, 1844
- Bensby T., Feltzing S., Lundström I., 2003, [A&A](#), **410**, 527
- Bensby T., Feltzing S., Lundström I., Ilyin I., 2005, [A&A](#), **433**, 185
- Bensby T., Feltzing S., Oey M. S., 2014, [A&A](#), **562**, A71
- Berta-Thompson Z. K., et al., 2015, [Nature](#), **527**, 204
- Boesgaard A. M., Friel E. D., 1990, [ApJ](#), **351**, 467
- Boesgaard A. M., Tripicco M. J., 1986, [ApJ](#), **303**, 724
- Bonfils X., Delfosse X., Udry S., Santos N. C., Forveille T., Ségransan D., 2005, [A&A](#), **442**, 635
- Bonnarel F., et al., 2000, [A&AS](#), **143**, 33
- Borgniet S., et al., 2014, [A&A](#), **561**, A65
- Brewer J. M., Fischer D. A., Valenti J. A., Piskunov N., 2016, [ApJS](#), **225**, 32
- Buchhave L. A., et al., 2012, [Nature](#), **486**, 375
- Buchhave L. A., Bitsch B., Johansen A., Latham D. W., Bizzarro M., Bieryla A., Kipping D. M., 2018, [ApJ](#), **856**, 37

- Burgasser A. J., et al., 2000, *ApJ*, **531**, L57
 Butler R. P., et al., 2006, *ApJ*, **646**, 505
 Caballero J. A., 2007, *ApJ*, **667**, 520
 Caballero J. A., 2009, *A&A*, **507**, 251
 Caballero J. A., et al., 2016, in 19th Cambridge Workshop on Cool Stars, Stellar Systems, and the Sun (CS19). p. 148, doi:10.5281/zenodo.600060
 Casagrande L., Flynn C., Bessell M., 2008, *MNRAS*, **389**, 585
 Catalá C., Forveille T., Lai O., 2006, *AJ*, **132**, 2318
 Charbonneau D., et al., 2009, *Nature*, **462**, 891
 Chen Y. Q., Nissen P. E., Zhao G., Zhang H. W., Benoni T., 2000, *A&AS*, **141**, 491
 Clanton C., Gaudi B. S., 2014, *ApJ*, **791**, 91
 Cortés-Conterras M., et al., 2017, *A&A*, **597**, A47
 Courcol B., et al., 2015, *A&A*, **581**, A38
 Cutri R. M., et al. 2014, VizieR Online Data Catalog, [2328](#)
 De Silva G. M., Freeman K. C., Bland-Hawthorn J., Asplund M., Bessell M. S., 2007, *AJ*, **133**, 694
 De Silva G. M., D’Orazi V., Melo C., Torres C. A. O., Gieles M., Quast G. R., Sterzik M., 2013, *MNRAS*, **431**, 1005
 Desidera S., et al., 2004, *A&A*, **420**, 683
 Dhital S., West A. A., Stassun K. G., Bochanski J. J., 2010, *AJ*, **139**, 2566
 Dittmann J. A., et al., 2017, *Nature*, **544**, 333
 Dumusque X., et al., 2011, *A&A*, **535**, A55
 Duquennoy A., Mayor M., 1991, *A&A*, **248**, 485
 Duquennoy A., Mayor M., Andersen J., Carquillat J. M., North P., 1992, *A&A*, **254**, L13
 Eggen O. J., 1984, *AJ*, **89**, 1358
 Eggen O. J., 1989, *PASP*, **101**, 366
 Eggen O. J., 1994, in Morrison L. V., Gilmore G. F., eds, Galactic and Solar System Optical Astrometry. p. 191
 Ehrenreich D., Lagrange A.-M., Montagnier G., Chauvin G., Galland F., Beuzit J.-L., Rameau J., 2010, *A&A*, **523**, A73
 Eisenbeiss T., Ammler-von Eiff M., Roell T., Mugrauer M., Adam C., Neuhäuser R., Schmidt T. O. B., Bedalov A., 2013, *A&A*, **556**, A53
 Epchtein N., et al., 1997, *The Messenger*, **87**, 27
 Faherty J. K., Burgasser A. J., Cruz K. L., Shara M. M., Walter F. M., Gelino C. R., 2009, *AJ*, **137**, 1
 Famaey B., Siebert A., Jorissen A., 2008, *A&A*, **483**, 453
 Favata F., Micela G., Sciortino S., 1997, *A&A*, **323**, 809
 Fischer D. A., Valenti J., 2005, *ApJ*, **622**, 1102
 Fischer D. A., et al., 2007, *ApJ*, **669**, 1336
 Fuhrmann K., 2004, *Astronomische Nachrichten*, **325**, 3
 Fuhrmann K., 2008, *MNRAS*, **384**, 173
 Fulbright J. P., 2000, *AJ*, **120**, 1841
 Gagné J., et al., 2018, *ApJ*, **856**, 23
 Gaia Collaboration et al., 2016, *A&A*, **595**, A1
 Gaia Collaboration Brown A. G. A., Vallenari A., Prusti T., de Bruijne J. H. J., Babusiaux C., Bailer-Jones C. A. L., 2018, preprint, ([arXiv:1804.09365](#))
 Gaidos E., Mann A. W., 2014, *ApJ*, **791**, 54
 Ghezzi L., Cunha K., Smith V. V., de Araújo F. X., Schuler S. C., de la Reza R., 2010, *ApJ*, **720**, 1290
 Gliese W., Jahreiß H., 1991, Technical report, Preliminary Version of the Third Catalogue of Nearby Stars
 Goldberg D., Mazeh T., Latham D. W., Stefanik R. P., Carney B. W., Laird J. B., 2002, *AJ*, **124**, 1132
 Goldin A., Makarov V. V., 2007, *ApJS*, **173**, 137
 Golimowski D. A., Nakajima T., Kulkarni S. R., Oppenheimer B. R., 1995, *ApJ*, **444**, L101
 González G., 1997, *MNRAS*, **285**, 403
 González G., 2006, *PASP*, **118**, 1494
 Gould A., Chanamé J., 2004, *ApJS*, **150**, 455
 Gratton R. G., Garretta E., Claudi R., Lucatello S., Barbieri M., 2003, *A&A*, **404**, 187
 Gray D. F., 2015, *ApJ*, **810**, 117
 Griffin R. F., 1994, *MNRAS*, **267**, 69
 Griffin R. F., 2001, *The Observatory*, **121**, 221
 Griffin R. F., 2002, *The Observatory*, **122**, 14
 Griffin R. F., 2003, *The Observatory*, **123**, 286
 Guillot T., Santos N. C., Pont F., Iro N., Melo C., Ribas I., 2006, *A&A*, **453**, L21
 Guillout P., et al., 2009, *A&A*, **504**, 829
 Halbwachs J.-L., Mayor M., Udry S., 2012, *MNRAS*, **422**, 14
 Hambly N. C., et al., 2001, *MNRAS*, **326**, 1279
 Hartkopf W. I., McAlister H. A., Mason B. D., Barry D. J., Turner N. H., Fu H.-H., 1994, *AJ*, **108**, 2299
 Hatzes A. P., et al., 2015, *A&A*, **580**, A31
 Hauschildt P. H., Baron E., 2010, *A&A*, **509**, A36
 Henry T. J., Jao W.-C., Subasavage J. P., Beaulieu T. D., Ianna P. A., Costa E., Méndez R. A., 2006, *AJ*, **132**, 2360
 Hobson M. J., Jofré E., García L., Petrucci R., Gómez M., 2018, *Rev. Mex. Astron. Astrofis.*, **54**, 65
 Högl E., et al., 2000, *A&A*, **355**, L27
 Horch E. P., Howell S. B., Everett M. E., Ciardi D. R., 2012, *AJ*, **144**, 165
 Horch E. P., van Belle G. T., Davidson Jr. J. W., Ciastko L. A., Everett M. E., Bjorkman K. S., 2015, *AJ*, **150**, 151
 Hui-Bon-Hoa A., 2000, *A&AS*, **144**, 203
 Ishigaki M. N., Chiba M., Aoki W., 2012, *ApJ*, **753**, 64
 Ivanov G. A., 2008, *Kinematika i Fizika Nebesnykh Tel*, **24**, 480
 Ivans I. I., Sneden C., James C. R., Preston G. W., Fulbright J. P., Höflich P. A., Carney B. W., Wheeler J. C., 2003, *ApJ*, **592**, 906
 Jancart S., Jorissen A., Babusiaux C., Pourbaix D., 2005, *A&A*, **442**, 365
 Janson M., et al., 2013, *ApJ*, **773**, 73
 Jofré P., et al., 2014, *A&A*, **564**, A133
 Jofré P., et al., 2015, *A&A*, **582**, A81
 Johnson J. A., Apps K., 2009, *ApJ*, **699**, 933
 Johnson D. R. H., Soderblom D. R., 1987, *AJ*, **93**, 864
 Johnson J. A., Aller K. M., Howard A. W., Crepp J. R., 2010, *PASP*, **122**, 905
 Johnson J. A., et al., 2012, *AJ*, **143**, 111
 Katoh N., Itoh Y., Toyota E., Sato B., 2013, *AJ*, **145**, 41
 Katz D., Soubiran C., Cayrel R., Barbuy B., Friel E., Bienaymé O., Perrin M.-N., 2011, *A&A*, **525**, A90
 Kim B., An D., Stauffer J. R., Lee Y. S., Terndrup D. M., Johnson J. A., 2016, *ApJS*, **222**, 19
 King J. R., Villarreal A. R., Soderblom D. R., Gulliver A. F., Adelman S. J., 2003, *AJ*, **125**, 1980
 Klutsch A., Freire Ferrero R., Guillout P., Frasca A., Marilli E., Montes D., 2014, *A&A*, **567**, A52
 Krisciunas K., et al., 1993, *MNRAS*, **263**, 781
 Kurucz R., 1993, ATLAS9 Stellar Atmosphere Programs and 2 km/s grid. Kurucz CD-ROM No. 13. Cambridge, Mass.: Smithsonian Astrophysical Observatory, 1993., 13
 Lafrenière D., et al., 2007, *ApJ*, **670**, 1367
 Lasker B. M., et al., 2008, *AJ*, **136**, 735
 Latham D. W., Mazeh T., Carney B. W., McCrosky R. E., Stefanik R. P., Davis R. J., 1988, *AJ*, **96**, 567
 Latham D. W., et al., 1992, *AJ*, **104**, 774
 Latham D. W., Stefanik R. P., Torres G., Davis R. J., Mazeh T., Carney B. W., Laird J. B., Morse J. A., 2002, *AJ*, **124**, 1144
 Laughlin G., Bodenheimer P., Adams F. C., 2004, *ApJ*, **612**, L73
 Le Borgne J.-F., et al., 2003, *A&A*, **402**, 433
 Lépine S., Bongiorno B., 2007, *AJ*, **133**, 889
 Lépine S., Rich R. M., Shara M. M., 2007, *ApJ*, **669**, 1235
 López-Santiago J., Montes D., Crespo-Chacón I., Fernández-Figueroa M. J., 2006, *ApJ*, **643**, 1160
 López-Santiago J., Montes D., Gálvez-Ortiz M. C., Crespo-Chacón I., Martínez-Arnáiz R. M., Fernández-Figueroa M. J., de Castro E., Cornide M., 2010, *A&A*, **514**, A97
 Luck R. E., 2017, *AJ*, **153**, 21
 Luck R. E., Heiter U., 2005, *AJ*, **129**, 1063
 Maldonado J., et al., 2015, *A&A*, **577**, A132
 Malo L., Doyon R., Feiden G. A., Albert L., Lafrenière D., Artigau É., Gagné J., Riedel A., 2014, *ApJ*, **792**, 37
 Mann A. W., Brewer J. M., Gaidos E., Lépine S., Hilton E. J., 2013, *AJ*, **145**, 52

- Mann A. W., Deacon N. R., Gaidos E., Ansdell M., Brewer J. M., Liu M. C., Magnier E. A., Aller K. M., 2014, *AJ*, **147**, 160
- Mann A. W., Feiden G. A., Gaidos E., Boyajian T., von Braun K., 2015, *AJ*, **804**, 64
- Martin D. V., 2018, preprint, ([arXiv:1802.08693](https://arxiv.org/abs/1802.08693))
- Mason B. D., Wycoff G. L., Hartkopf W. I., Douglass G. G., Worley C. E., 2001, *AJ*, **122**, 3466
- Mazeh T., Simon M., Prato L., Markus B., Zucker S., 2003, *ApJ*, **599**, 1344
- McDonald I., Zijlstra A. A., Watson R. A., 2017, *MNRAS*, **471**, 770
- Mishenina T. V., Soubiran C., Kovtyukh V. V., Korotin S. A., 2004, *A&A*, **418**, 551
- Mishenina T. V., Soubiran C., Kovtyukh V. V., Katsova M. M., Livshits M. A., 2012, *A&A*, **547**, A106
- Monet D., 1998, USNO-A2.0
- Montes D., 2010, *Highlights of Astronomy*, **15**
- Montes D., 2015, in Cenarro A. J., Figueiras F., Hernández-Monteagudo C., Trujillo Bueno J., Valdvielso L., eds, *Highlights of Spanish Astrophysics VIII*. pp 606–606
- Montes D., López-Santiago J., Gálvez M. C., Fernández-Figueroa M. J., De Castro E., Cornide M., 2001, *MNRAS*, **328**, 45
- Muiños J. L., Evans D. W., 2014, *Astronomische Nachrichten*, **335**, 367
- Nelson B. E., Ford E. B., Wright J. T., Fischer D. A., von Braun K., Howard A. W., Payne M. J., Dindar S., 2014, *MNRAS*, **441**, 442
- Neves V., Santos N. C., Sousa S. G., Correia A. C. M., Israeli G., 2009, *A&A*, **497**, 563
- Neves V., et al., 2012, *A&A*, **538**, A25
- Neves V., Bonfils X., Santos N. C., Delfosse X., Forveille T., Allard F., Udry S., 2014, *A&A*, **568**, A121
- Newton E. R., Charbonneau D., Irwin J., Berta-Thompson Z. K., Rojas-Ayala B., Covey K., Lloyd J. P., 2014, *AJ*, **147**, 20
- Oh S., Price-Whelan A. M., Brewer J. M., Hogg D. W., Spergel D. N., Myles J., 2018, *ApJ*, **854**, 138
- Önehag A., Heiter U., Gustafsson B., Piskunov N., Plez B., Reiners A., 2012, *A&A*, **542**, A33
- Pasquini L., Döllinger M. P., Weiss A., Girardi L., Chavero C., Hatzes A. P., da Silva L., Setiawan J., 2007, *A&A*, **473**, 979
- Passegger V. M., et al., 2018, preprint, ([arXiv:1802.02946](https://arxiv.org/abs/1802.02946))
- Paulson D. B., Yelda S., 2006, *PASP*, **118**, 706
- Paulson D. B., Sneden C., Cochran W. D., 2003, *AJ*, **125**, 3185
- Perrier C., Sivan J.-P., Naef D., Beuzit J. L., Mayor M., Queloz D., Udry S., 2003, *A&A*, **410**, 1039
- Perryman M. A. C., et al., 1997, *A&A*, **323**, L49
- Pompéia L., et al., 2011, *MNRAS*, **415**, 1138
- Pourbaix D., et al., 2004, *A&A*, **424**, 727
- Poveda A., Herrera M. A., Allen C., Cordero G., Lavallee C., 1994, *Rev. Mex. Astron. Astrofis.*, **28**, 43
- Poveda A., Allen C., Costero R., Echevarría J., Hernández-Alcántara A., 2009, *ApJ*, **706**, 343
- Prieur J.-L., Scardia M., Pansecchi L., Argyle R. W., Zanutta A., Aristidi E., 2014, *Astronomische Nachrichten*, **335**, 817
- Prugniel P., Vauglin I., Koleva M., 2011, *A&A*, **531**, A165
- Quirrenbach A., et al., 2016, in SPIE, Ground-based and Airborne Instrumentation for Astronomy VI. p. 990812, doi:[10.1117/12.2231880](https://doi.org/10.1117/12.2231880)
- Raghavan D., et al., 2010, *ApJS*, **190**, 1
- Ramírez I., Fish J. R., Lambert D. L., Allende Prieto C., 2012, *ApJ*, **756**, 46
- Ramírez I., Allende Prieto C., Lambert D. L., 2013, *ApJ*, **764**, 78
- Ramírez I., et al., 2014, *A&A*, **572**, A48
- Randich S., Pallavicini R., Meola G., Stauffer J. R., Balachandran S. C., 2001, *A&A*, **372**, 862
- Raskin G., et al., 2011, *A&A*, **526**, A69
- Reiners A., et al., 2018, *A&A*, **612**, A49
- Riedel A. R., Blunt S. C., Lambrides E. L., Rice E. L., Cruz K. L., Faherty J. K., 2017, *AJ*, **153**, 95
- Robertson P., et al., 2012, *ApJ*, **749**, 39
- Robinson S. E., Ammons S. M., Kretke K. A., Strader J., Wertheimer J. G., Fischer D. A., Laughlin G., 2007, *ApJS*, **169**, 430
- Roederer I. U., Preston G. W., Thompson I. B., Shectman S. A., Sneden C., Burley G. S., Kelson D. D., 2014, *AJ*, **147**, 136
- Roeser S., Demleitner M., Schilbach E., 2010, *AJ*, **139**, 2440
- Rojas-Ayala B., Covey K. R., Muirhead P. S., Lloyd J. P., 2010, *ApJ*, **720**, L113
- Rojas-Ayala B., Covey K. R., Muirhead P. S., Lloyd J. P., 2012, *ApJ*, **748**, 93
- Salim S., Gould A., 2003, *ApJ*, **582**, 1011
- Sandage A., 1969, *ApJ*, **158**, 1115
- Santos N. C., Israeli G., Mayor M., 2001, *A&A*, **373**, 1019
- Santos N. C., Israeli G., Mayor M., 2004, *A&A*, **415**, 1153
- Santos N. C., Israeli G., Mayor M., Bento J. P., Almeida P. C., Sousa S. G., Ecuvillon A., 2005, *A&A*, **437**, 1127
- Santos N. C., et al., 2013, *A&A*, **556**, A150
- Schlaufman K. C., Laughlin G., 2010, *A&A*, **519**, A105
- Schlieder J. E., Lépine S., Simon M., 2012, *AJ*, **143**, 80
- Schröder C., Reiners A., Schmitt J. H. M. M., 2009, *A&A*, **493**, 1099
- Shkolnik E. L., Allers K. N., Kraus A. L., Liu M. C., Flagg L., 2017, *AJ*, **154**, 69
- Simons D. A., Henry T. J., Kirkpatrick J. D., 1996, *AJ*, **112**, 2238
- Skrutskie M. F., et al., 2006, *AJ*, **131**, 1163
- Smiljanic R., 2012, *MNRAS*, **422**, 1562
- Sneden C. A., 1973, PhD thesis, The University of Texas at Austin.
- Soubiran C., Katz D., Cayrel R., 1998, *A&AS*, **133**, 221
- Soubiran C., Le Campion J.-F., Brouillet N., Chemin L., 2016, *A&A*, **591**, A118
- Sousa S. G., Santos N. C., Israeli G., Mayor M., Monteiro M. J. P. F. G., 2006, *A&A*, **458**, 873
- Sousa S. G., et al., 2008, *A&A*, **487**, 373
- Sousa S. G., Santos N. C., Israeli G., Mayor M., Udry S., 2011, *A&A*, **533**, A141
- Sousa S. G., Santos N. C., Adibekyan V., Delgado-Mena E., Israeli G., 2015, *A&A*, **577**, A67
- Southworth J., 2010, *MNRAS*, **408**, 1689
- Souto D., et al., 2017, *ApJ*, **835**, 239
- Spada F., Demarque P., Kim Y.-C., Boyajian T. S., Brewer J. M., 2017, *ApJ*, **838**, 161
- Stephens A., Boesgaard A. M., 2002, *AJ*, **123**, 1647
- Tabernero H. M., Montes D., González Hernández J. I., 2012, *A&A*, **547**, A13
- Tabernero H. M., Montes D., González Hernández J. I., Ammler-von Eiff M., 2017, *A&A*, **597**, A33
- Takeda Y., Ohkubo M., Sato B., Kambe E., Sadakane K., 2005, *PASJ*, **57**, 27
- Taylor M. B., 2005, in Shopbell P., Britton M., Ebert R., eds, *Astronomical Society of the Pacific Conference Series Vol. 347, Astronomical Data Analysis Software and Systems XIV*. p. 29
- Terrien R. C., Mahadevan S., Bender C. F., Deshpande R., Ramsey L. W., Bochanski J. J., 2012, *ApJ*, **747**, L38
- Teske J. K., Ghezzi L., Cunha K., Smith V. V., Schuler S. C., Bergemann M., 2015, *ApJ*, **801**, L10
- Tokovinin A. A., 1997, *A&AS*, **124**, 75
- Tokovinin A., Kiyaeva O., 2016, *MNRAS*, **456**, 2070
- Tomkin J., Lambert D. L., 1999, *ApJ*, **523**, 234
- Torres C. A. O., Quast G. R., Melo C. H. F., Sterzik M. F., 2008, *Young Nearby Loose Associations*. p. 757
- Torres C. A. O., Quast G. R., Montes D., 2016, in Kastner J. H., Stelzer B., Metchev S. A., eds, *IAU Symposium Vol. 314, Young Stars Planets Near the Sun*. pp 77–78 ([arXiv:1510.03067](https://arxiv.org/abs/1510.03067)), doi:[10.1017/S1743921315006596](https://doi.org/10.1017/S1743921315006596)
- Tsantaki M., Sousa S. G., Adibekyan V. Z., Santos N. C., Mortier A., Israeli G., 2013, *A&A*, **555**, A150
- Valenti J. A., Fischer D. A., 2005, *ApJS*, **159**, 141
- Valenti J. A., Piskunov N., Johns-Krull C. M., 1998, *ApJ*, **498**, 851
- Valls-Gabaud D., 1988, *L'Astronomie*, **102**, 493
- Vauclair S., Laymand M., Bouchy F., Vauclair G., Hui Bon Hoa A., Charpinet S., Bazot M., 2008, *A&A*, **482**, L5
- Vogt S. S., Butler R. P., Marcy G. W., Fischer D. A., Henry G. W., Laughlin G., Wright J. T., Johnson J. A., 2005, *ApJ*, **632**, 638
- Wallerstein G., 1973, *PASP*, **85**, 115
- Wang J., Ford E. B., 2011, *MNRAS*, **418**, 1822

- West A. A., Bochanski J. J., Bowler B. P., Dotter A., Johnson J. A., Lépine S., Rojas-Ayala B., Schweitzer A., 2011, in Johns-Krull C., Browning M. K., West A. A., eds, Astronomical Society of the Pacific Conference Series Vol. 448, 16th Cambridge Workshop on Cool Stars, Stellar Systems, and the Sun. p. 531 ([arXiv:1101.1086](https://arxiv.org/abs/1101.1086))
- Woolf V. M., Wallerstein G., 2005, *MNRAS*, **356**, 963
- Woolf V. M., Wallerstein G., 2006, *PASP*, **118**, 218
- Woolf V. M., West A. A., 2012, *MNRAS*, **422**, 1489
- Woolf V. M., Lépine S., Wallerstein G., 2009, *PASP*, **121**, 117
- Wright J. T., Upadhyay S., Marcy G. W., Fischer D. A., Ford E. B., Johnson J. A., 2009, *ApJ*, **693**, 1084
- Wright N. J., Drake J. J., Mamajek E. E., Henry G. W., 2011, *ApJ*, **743**, 48
- Zacharias N., Finch C. T., Girard T. M., Henden A., Bartlett J. L., Monet D. G., Zacharias M. I., 2012, VizieR Online Data Catalog, [1322](#)
- Zacharias N., Finch C., Frouard J., 2017, VizieR Online Data Catalog, [1340](#)
- Zapatero Osorio M. R., Martín E. L., 2004, *A&A*, **419**, 167
- Zhang Z. H., et al., 2013, *MNRAS*, **434**, 1005
- Zuckerman B., Song I., 2004, *ARA&A*, **42**, 685
- da Silva R., Milone A. d. C., Rocha-Pinto H. J., 2015, *A&A*, **580**, A24
- Ženovič R., Tautvaišienė G., Nordström B., Stokutė E., 2014, *A&A*, **563**, A53
- van Altena W. F., Lee J. T., Hoffleit D., 1995, VizieR Online Data Catalog, [1174](#)
- van Leeuwen F., 2007, *A&A*, **474**, 653

APPENDIX A: ADDITIONAL GRAPHS

APPENDIX B: LONG TABLES

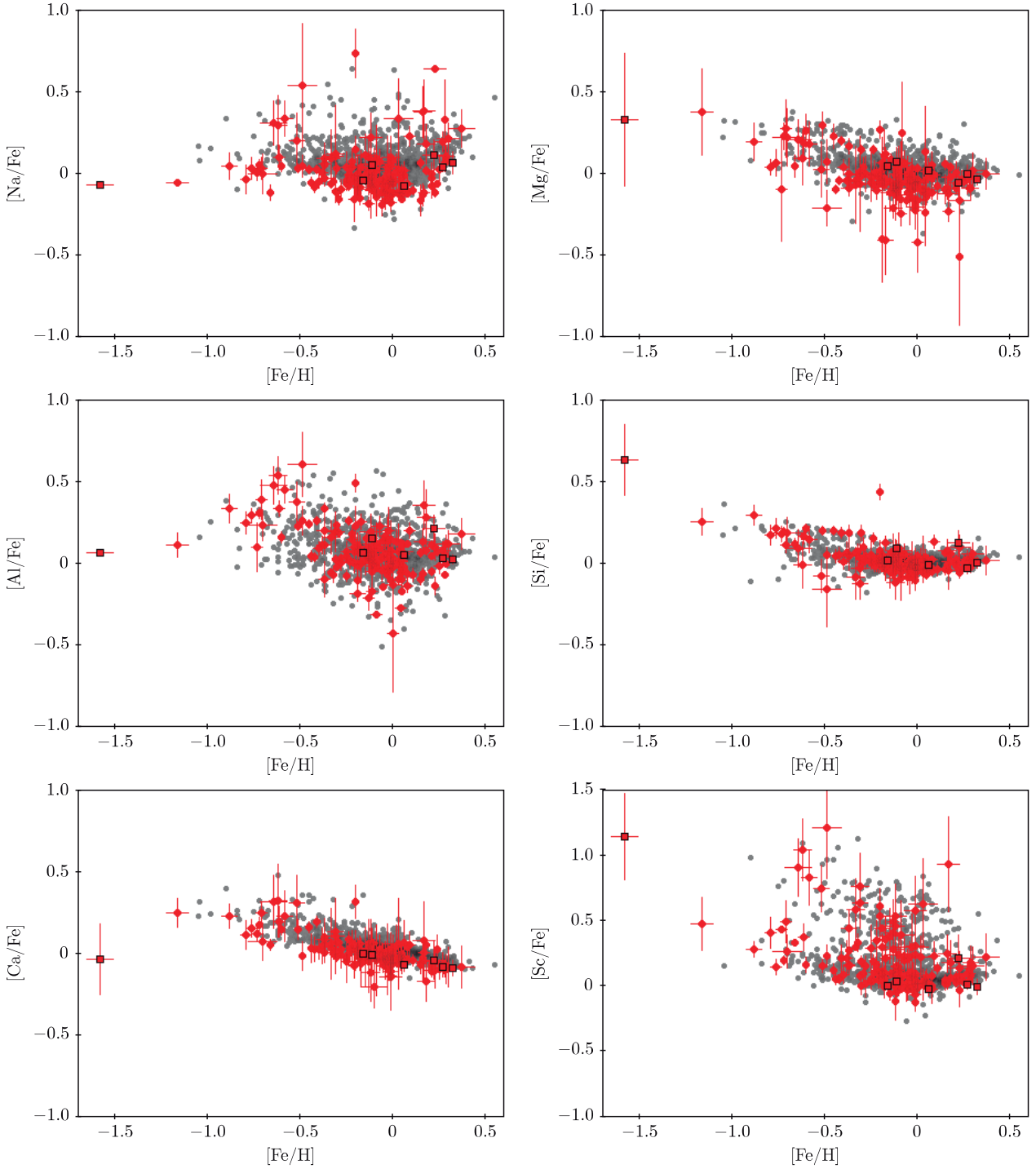


Figure A1. Abundance ratios of $[X/\text{Fe}]$ versus $[\text{Fe}/\text{H}]$, where $X = \text{Na}, \text{Mg}, \text{Al}, \text{Si}, \text{Ca}$, and Sc . Red circles: our stars; black-ensquared circles: low-gravity stars; small grey circles: stars from Adibekyan et al. (2012).

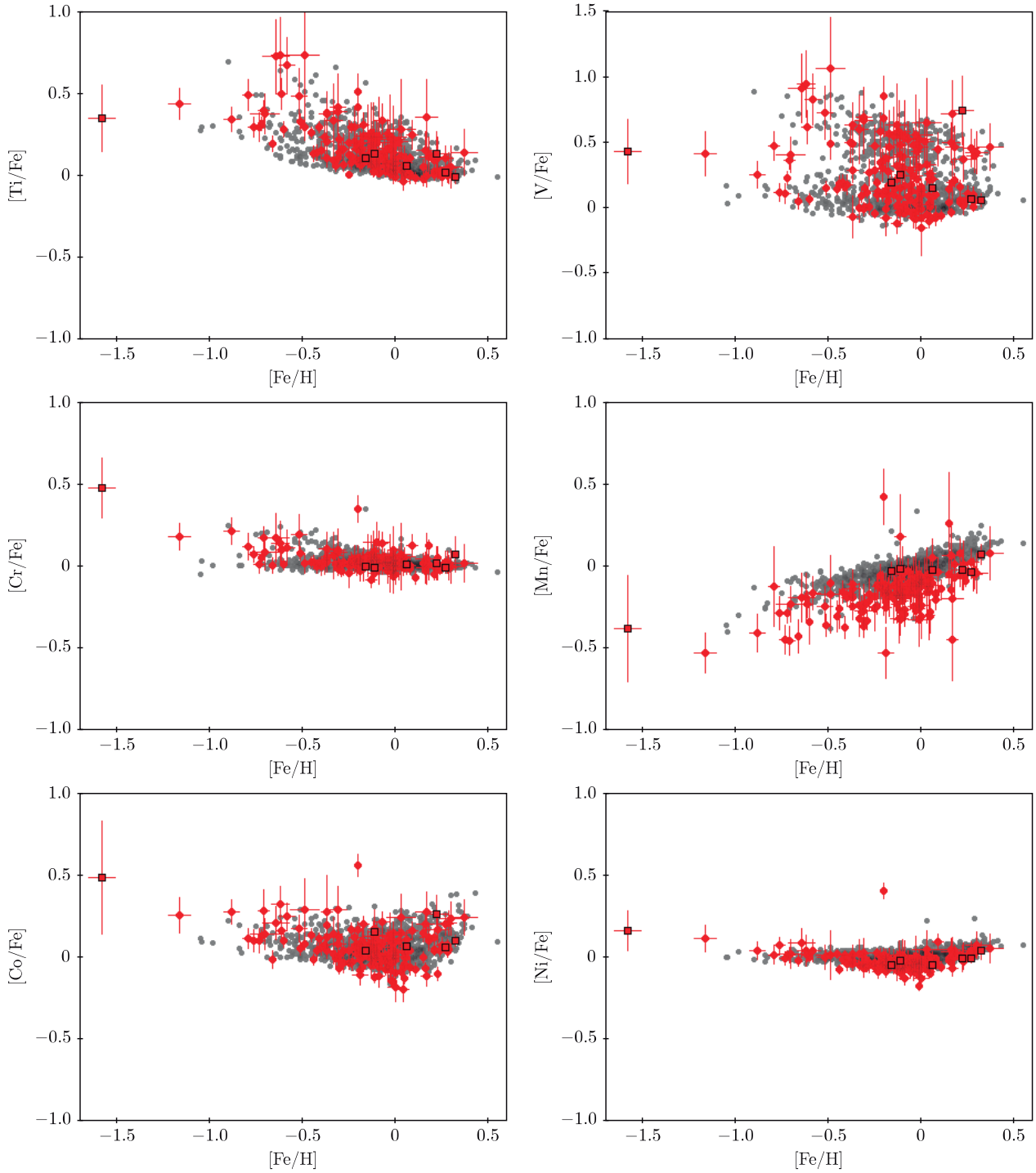
**Figure A2.** Same as Fig. A1, but for X = Ti, V, Cr, Mn, Co, and Ni.

Table B1. Basic properties of investigated systems and stars.

WDS	Comp.	Discoverer code	ρ [arcsec]	θ [deg]	Name ^a	α (J2000)	δ (J2000)	J^b [mag]	Spectral type	Obs. ^c
00153+5304	A				G 217-41	00:15:14.8	+53:04:27	8.84±0.02	K3 V	H
	B	GIC 5	18.90±0.08	354.43±0.23	G 217-40	00:15:14.6	+53:04:46	10.82±0.02	M2.5 V	C
00385+4300	A				BD+42 126	00:38:29.2	+43:00:00	8.41±0.02	G5 V	H
	B	LDS 5176	53.09±0.08	124.45±0.02	LP 193-345	00:38:33.2	+42:59:30	10.49±0.02	M0.5 V	C*
00452+0015	A				HD 4271 Aa,Ab	00:45:11.0	+00:15:12	5.98±0.02	F8 V	H
	BC	LDS 836	55.35±0.17	44.90±0.24	HD 4271 B	00:45:13.6	+00:15:51	10.11±0.02	M4.0 V+	C
00467-0426 ^d	Aa,Ab				HD 4449	00:46:40.5	-04:25:37	6.09±0.02	G5 V	H
	B	LDS 9100	66.80±0.10	39.41±0.12	LP 646-9	00:46:43.4	-04:24:46	11.12±0.03	M4.0 V	C
00491+5749	A				Achird Aa,Ab	00:49:06.2	+57:48:55	2.11±0.57	G0 V	H
	B	STF 60	12.49±0.34	317.53±0.09	η Cas B	00:49:05.2	+57:49:04	7.17	K7 V	C
	C	STF 60	225.06±0.30	259.50±0.09	Zkh 17	00:48:38.5	+57:48:14	9.55±0.02
01055+1523	A				HD 6440 A	01:05:29.9	+15:23:24	7.12±0.02	K3.5 V	H
	B	STF 87	6.15±0.23	202.66±2.81	HD 6440 B	01:05:29.8	+15:23:18	7.15±0.02	K7 V	C
01076+2257	A				HD 6660 A	01:07:37.9	+22:57:19	6.42±0.02	K4 V	H
	B	LDS 9112	9.54±0.10	72.54±0.75	HD 6660 B	01:07:38.5	+22:57:22	9.53±0.04	M3.5 V	C
01187-0052	Aa,Ab				HD 7895	01:18:41.1	-00:52:03	6.54±0.02	K0 V+	H
	B	HJ 5453	27.93±0.18	208.46±0.51	HD 7895 B	01:18:40.2	-00:52:28	8.01±0.02	K7 V	C
	C	HJ 5453	251.54±0.18	17.35±0.05	J01184607-0048029	01:18:46.1	-00:48:03	12.39±0.02
01215+3120	A				EN Psc	01:21:28.2	+31:20:29	6.81±0.02	K2 V	H
	B	LDS 1096	10.42±0.08	290.88±0.27	BD+30 206B	01:21:27.4	+31:20:33	9.98±0.02	M3.5 V	C
01226+1245	A				BD+12 168A	01:22:36.6	+12:45:04	7.86±0.03	K3 V	H
	B	BU 1360	5.71±0.11	24.41±1.49	BD+12 168B	01:22:36.7	+12:45:09	8.68±0.03	K7 V	C*
01230-1258	A				HD 8389 A	01:23:02.6	-12:57:58	6.40±0.02	K0 V	H
	BC	GAL 307	40.79±0.08	313.17±0.01	HD 8389 B	01:23:00.6	-12:57:30	8.75±0.02	M0.0 V+	C*
01340-0141	A				BD-02 247	01:34:02.1	-01:41:10	8.65±0.02	G5 V	H
	B	SKF 296	431.96±0.11	20.82±0.02	LP 588-9	01:34:12.4	-01:34:26	11.72±0.02	M1.0 V	C
01450-0104	A				BD-01 237	01:44:59.1	-01:03:31	8.29±0.03	K0 V	H
	B	LDS 9123	41.57±0.13	310.54±0.02	LP 588-44	01:44:57.0	-01:03:04	11.03±0.02	M2.0	C*
01572-1015	A				HD 11964 A	01:57:09.6	-10:14:33	5.02±0.03	G8 IV	H
	B	GAL 315	29.65±0.36	133.74±0.02	HD 11964 B	01:57:11.0	-10:14:53	8.41±0.02	M0.0 V	C
02290-1959	Aa,Ab				HD 15468	02:29:01.7	-19:58:45	6.59±0.02	K4 V+	H
	B	UC 744	474.31±0.11	242.16±0.02	HD 15468 C	02:28:31.9	-20:02:27	9.18±0.03	M2.5 V	C
02291+2252	A				BD+22 353Aa,Ab	02:29:07.3	+22:52:05	7.84±0.02	K0 V	H
	B	HU 603	5.85±0.08	231.41±1.16	BD+22 353B	02:29:07.0	+22:52:01	8.73±0.03	K7 V	C
	C	HU 603	78.98±0.09	272.15±0.06	J02290160+2252084	02:29:01.6	+22:52:08	10.26±0.02
	D	FOX 9043	46.55±0.08	259.94±0.12	J02290400+2251573	02:29:04.0	+22:51:57	12.94±0.02
02361+0653 ^e	AB				HD 16160 A	02:36:04.9	+06:53:13	4.15±0.26	K0 V+	H
	C	PLQ 32	163.95±0.33	109.55±0.07	BX Cet	02:36:15.4	+06:52:19	7.33±0.02	M4.0 V	C
02442+4914	A				θ Per A	02:44:12.0	+49:13:42	3.03±0.24	F7 V	H
	B	STF 296	20.52±0.30	304.76±0.20	θ Per B	02:44:10.3	+49:13:54	6.69±0.02	M1.5 V	C
	C	STF 296	94.35±0.30	242.67±0.24	J02440341+4912590	02:44:03.4	+49:12:59	10.61±0.02
02482+2704	A				BC Ari Aa,Ab	02:48:09.1	+27:04:07	6.06±0.03	K1 V	H
	B	LDS 1138	20.33±0.08	22.48±0.31	LP 354-414	02:48:09.7	+27:04:26	10.73±0.02	M5 V	C*
02556+2652	A				HD 18143 A	02:55:39.1	+26:52:24	6.90±0.04	K2 IV	H
	B	STF326	5.27±0.11	220.98±1.74	HD 18143 B	02:55:38.8	+26:52:20	6.89±0.04	K7 V	...
	C	LDS 883	43.95±0.11	265.70±0.16	HD 18143 C	02:55:35.8	+26:52:21	9.56±0.02	M4.0 V	C
03042+6142	A				HD 18757	03:04:09.6	+61:42:21	5.39±0.02	G4 V	H
	B	KUI 11	55.54±0.09	313.65±0.01	J03040397+6142596	03:04:04.0	+61:43:00	10.87±0.02
	C	LDS 9142	263.08±0.08	65.67±0.02	vMa 2-4	03:04:43.4	+61:44:10	8.88±0.02	M3.0 V	C
03078+2533	A				HD 19381 A	03:07:50.5	+25:33:07	7.23±0.02	F8 V	H
	B	TOK 234	124.12±0.08	122.09±0.01	HD 19381 B	03:07:58.3	+25:32:02	11.25±0.02	M3.5 V	C*
03150+0101	A				BD+00 549A	03:15:04.8	+01:02:15	8.91±0.02	G5 V	H
	B	GIC 39	78.18±0.10	312.69±0.01	BD+00 549B	03:15:00.9	+01:03:08	11.62±0.03	M0.5 V	C*
03206+0902	A				HD 20727 Aa,Ab	03:20:37.0	+09:02:01	7.11±0.02	G0 V	H
	B	GIC 40	81.65±0.11	83.53±0.08	HD 20727 B	03:20:42.5	+09:02:10	11.08±0.02	M4.0 V	C*

Table B1 – continued Basic properties of investigated systems and stars.

WDS	Comp.	Discoverer code	ρ [arcsec]	θ [deg]	Name ^a	α (J2000)	δ (J2000)	J^b [mag]	Spectral type	Obs. ^c
03321+4340	A				HD 21727 A	03:32:05.1	+43:40:12	7.34±0.02	G5 V	H
	B	LDS 9155	14.50±0.08	136.91±0.02	HD 21727 B	03:32:05.9	+43:40:01	9.24±0.02	K7 V	C
03332+4615	A				V577 Per	03:33:13.5	+46:15:27	6.84±0.02	G5 V	H
	B	ES 560	9.46±0.08	142.28±0.09	HD 21845 B	03:33:14.0	+46:15:19	8.38±0.03	M0.0 V	C
03356+4253	A				HD 22122	03:35:35.8	+42:53:15	6.30±0.02	F8 V	H
	B	BUP 45	46.02±0.08	212.36±0.15	J03353356+4252364	03:35:33.6	+42:52:36	12.38±0.02
	C	BUP 45	180.33±0.09	90.95±0.03	HD 22157	03:35:52.2	+42:53:12	5.91±0.02	K0	...
	D	LDS 9156	82.39±0.08	283.78±0.04	Wolf 191	03:35:28.5	+42:53:35	10.83±0.02	M0.5 V	C
03396+1823	A				V1082 Tau Aa,Ab	03:39:33.6	+18:23:06	6.65±0.02	G5+	H
	B	TOK 14	9.89±0.18	245.35±1.35	J03393295+1823017	03:39:33.0	+18:23:02	11.86±0.06
	Ca,Cb	LDS 9159	254.74±0.18	175.73±0.03	Wolf 209	03:39:34.9	+18:18:52	9.33±0.02	M1.5 V	C*
03398+3328	A				HD 278874 Aa,Ab	03:39:49.0	+33:28:24	7.12±0.02	K2	H
	B	ES 327	15.43±0.10	294.46±0.18	HD 278874 B	03:39:47.9	+33:28:30	8.97±0.03	M3.0 V	C*
03480+4032	A				HD 23596	03:48:00.4	+40:31:50	6.17±0.02	F8 V	H
	B	TOK 240	70.79±0.08	62.81±0.09	J03480588+4032226	03:48:05.9	+40:32:23	9.35±0.02	M1.5 V	C
03520+3947	A				HD 275867	03:52:00.3	+39:47:44	7.55±0.02	K2 V	H
	B	GRV 197	53.82±0.08	207.48±0.12	TYC 2868-639-1	03:51:58.1	+39:46:57	8.28±0.02	M0.0 V	C
03556+5214	A				HD 24421	03:55:37.1	+52:13:37	5.77±0.03	F8 V	H
	B	LEP 16	52.39±0.08	358.12±0.08	LSPM J0355+5214	03:55:36.9	+52:14:29	10.89±0.03	M2.5 V	C
	C	LEP 16	236.57±0.09	191.39±0.03	LSPM J0355+5209	03:55:32.0	+52:09:45	11.18±0.02
03566+5042	A				43 Per Aa,Ab	03:56:36.5	+50:41:43	4.23±0.21	F5 V	H
	B	S 440	75.52±0.10	30.77±0.10	BD+50 860B	03:56:40.6	+50:42:48	8.15±0.02	K7 V	C
	C	S 440	88.49±0.10	132.16±0.01	J03564340+5040438 ^f	03:56:43.4	+50:40:44	11.35±0.02
	D	S 440	65.69±0.10	289.77±0.05	J03562999+5042055	03:56:30.0	+50:42:06	12.00±0.02
03575-0110	A				HD 24916 A	03:57:28.7	-01:09:34	6.06±0.02	K4 V	H
	B	BU 543	11.04±0.11	16.32±0.72	HD 24916 B	03:57:28.9	-01:09:23	7.77±0.02	M2.5 V	C
04153-0739	A				σ^2 Eri A	04:15:16.3	-07:39:10	3.01±0.24	K0.5 V	H
	B	STF 518	83.22±0.39	102.93±0.20	σ^2 Eri B	04:15:22.0	-07:39:25	9.85±0.03	DA2.9	...
	C	STF 518	78.34±0.39	97.71±0.25	σ^2 Eri C	04:15:21.7	-07:39:17	6.747±0.02	M4.5 V	C
04252+2545	A				HD 27887 A	04:25:10.8	+25:44:57	6.93±0.02	F5	H
	B	TOK 247	42.93±0.08	271.24±0.11	HD 27887 B	04:25:07.6	+25:44:58	11.51±0.02	M2.0 V	C*
04359+1631	A				Aldebaran	04:35:55.2	+16:30:33	-2.10±0.19	K5 III	H
	B ^g	BU 550	28.05±0.32	115.64±0.31	Aldebaran B	04:35:57.2	+16:30:21	...	M3.0 V	C*
	C	STB 2	133.16±0.32	31.36±0.19	BD+16 630	04:36:00.1	+16:32:27	8.36±0.06	K4	...
04397+0952	Aa,Ab				HD 286955	04:39:42.6	+09:52:19	7.15±0.02	K2 V+	H
	B	GIC 51	34.07±0.10	163.35±0.11	BD+09 621B	04:39:43.3	+09:51:47	10.26±0.02	M3.0 V	C*
04429+1843	A				HD 29836	04:42:51.7	+18:43:14	5.90±0.02	G2 V	H
	B	LDS 2266	141.76±0.08	102.94±0.02	HD 285970	04:43:01.4	+18:42:42	7.75±0.04	K5 V	C
	C	LDS 2266	301.65±0.08	119.43±0.01	LP 415-358	04:43:10.2	+18:40:46	12.35±0.03
04559+0440	Aa,Ab				HD 31412	04:55:55.9	+04:40:14	5.97±0.02	F9.5 V+	H
	B	LDS 9181	21.61±0.08	277.59±0.19	HD 31412 B	04:55:54.5	+04:40:16	8.50±0.02	M2.0 V	C
05003+2508	A				HD 31867 A	05:00:17.5	+25:08:11	6.81±0.03	G2 V	H
	B	TOK 253	33.96±0.10	126.52±0.04	HD 31867 B	05:00:19.5	+25:07:51	9.41±0.03	M1.0 V	C
05067+5136 ^h	AB				9 Aur Aa,Ab	05:06:40.6	+51:35:52	3.99±0.21	F2 V+M2	H
	C	H 6 35	90.13±0.17	61.59±0.15	9 Aur C	05:06:49.2	+51:36:35	7.34±0.03	K5 V	C
	D	BU 1046	143.57±0.17	350.79±0.06	J05063820+5138136	05:06:38.2	+51:38:14	10.58±0.02
05189-2124	A				HD 34751 A	05:18:47.2	-21:23:38	6.94±0.03	K6 V	H
	B	DON 101	4.91±0.08	76.38±1.21	HD 34751 B	05:18:47.5	-21:23:36	7.85±0.16	M3.5 V	C
05264+0351	A				HD 35638	05:26:23.1	+03:51:24	6.78±0.02	F5 V	H
	B	TOK 254	43.24±0.08	253.08±0.14	J05262029+0351111	05:26:20.3	+03:51:11	10.93±0.02	M1.5 V	C*
05289+1233	A				HD 35956 Aa,Ab	05:28:51.6	+12:33:03	5.61±0.02	G0 V	H
	B	TOK 94	5.56±0.08	71.04±1.12	J05285199+1233049	05:28:52.0	+12:33:05	7.59±0.08
	C	TOK 94	8.55±0.08	3.04±0.59	J05285166+1233117	05:28:51.7	+12:33:12	10.35±0.08
	D	TOK 94	16.86±0.08	245.12±0.38	J05285058+1232560	05:28:50.6	+12:32:56	9.18±0.02
	E	LDS 6186	99.39±0.10	134.17±0.01	G 102-4	05:28:56.5	+12:31:54	9.65±0.02	M4.0 V	C

Table B1 – continued Basic properties of investigated systems and stars.

WDS	Comp.	Discoverer code	ρ [arcsec]	θ [deg]	Name ^a	α (J2000)	δ (J2000)	J^b [mag]	Spectral type	Obs. ^c
05413+5329	A				V538 Aur	05:41:20.3	+53:28:52	4.30±0.26	K1 V	H
	B	ENG 22	98.04±0.13	71.24±0.09	HD 233153	05:41:30.7	+53:29:23	6.59±0.02	M1.0 V	C
	C	BUP 82	115.14±0.13	322.68±0.01	J05411251+5330239	05:41:12.5	+53:30:24	13.25±0.02
	D	BUP 82	697.49±0.13	282.57±0.01	HD 37229	05:40:04.0	+53:31:24	8.40±0.03	F5	...
05427+0241	A				HD 38014	05:42:45.8	+02:40:45	6.97±0.02	K1 V	H
	B	LDS 6192	57.07±0.14	354.91±0.13	G 99-27	05:42:45.5	+02:41:42	9.45±0.03	M3.0 V	C
05445-2227	A				γ Lep	05:44:27.8	-22:26:54	2.80±0.27	F6 V	H
	B	H 6 40	96.90±0.41	349.66±0.19	AK Lep	05:44:26.5	-22:25:19	4.85±0.19	K2 V	H
	C	H 5 50	206.60±0.30	0.42±0.08	J05442769-2223272	05:44:27.7	-22:23:27	10.35±0.03
	"D"	... ⁱ	1123.54±0.30	68.57±0.02	vB 1	05:45:43.2	-22:20:04	11.13±0.03	M3.5 V	C
05466+0110	A				HD 38529 A	05:46:34.9	+01:10:05	4.91±0.23	G4 IV	H
	B	RAG 1	283.82±0.14	304.77±0.01	HD 38529 B	05:46:19.4	+01:12:47	9.72±0.02	M2.5 V	C
05584-0439	AB				HD 40397 A	05:58:21.5	-04:39:02	5.66±0.02	G7 V	H
	C	A 322	194.46±0.08	302.67±0.01	HD 40374	05:58:10.6	-04:37:17	8.26±0.03	G5V	...
	D	LDS 3684	89.29±0.08	313.03±0.01	LP 659-4	05:58:17.2	-04:38:01	11.11±0.02	M4.5 V	C
06066+0431	A				Ross 413	06:06:30.0	+04:30:41	8.94±0.02	K4 V	H
	B	VBS 12	12.22±0.08	135.11±0.01	vB 2	06:06:30.6	+04:30:33	11.16±0.02	M3.0 V	C
06173+0506	Aa,Ab				HD 43587	06:17:16.1	+05:06:00	4.96±0.27	F9 V	H
	B	ENG 26	179.97±0.14	240.48±0.06	HD 254595	06:17:05.7	+05:04:31	9.45±0.02
	C	BUP 87	44.13±0.14	245.60±0.25	J06171345+0505419	06:17:13.4	+05:05:42	10.38±0.03
	D	BUP 87	67.62±0.14	212.41±0.17	J06171372+0505030	06:17:13.7	+05:05:03	11.95±0.03
	Ea,Eb	LEP 24	103.10±0.14	307.16±0.02	G 106-36	06:17:10.6	+05:07:02	9.09±0.02	M3.5 V+	C
06314-0134	A				HD 291763	06:31:23.1	-01:34:14	8.42±0.03	K2 V	H
	B	SKF 289	434.25±0.08	169.27±0.01	LHS 6107	06:31:28.5	-01:41:20	10.55±0.03	M1.5 V	C
06319+0039	A				HD 291725	06:31:51.4	+00:38:59	8.16±0.03	G7 V	H
	B	GIC 62	436.48±0.08	251.99±0.01	NLTT 16628	06:31:23.7	+00:36:45	11.08±0.02	M1.5 V	C
06332+0528	A				HD 46375 A	06:33:12.6	+05:27:47	6.45±0.02	K1 V	H
	B	SLE 299	10.43±0.08	310.09±0.03	HD 46375 B	06:33:12.1	+05:27:53	8.70±0.03	M2.0 V	C
06368+3751	A				BD+37 1545	06:36:46.4	+37:51:07	8.07±0.02	G5 V	H
	B	LEP 25	45.23±0.08	303.92±0.03	LSPM J0636+3751W	06:36:43.2	+37:51:32	11.44±0.03	M3.5 V	C
06461+3233	A				HD 263175 A	06:46:05.1	+32:33:20	7.02±0.02	K3 V	H
	B	LDS 6201	30.93±0.08	100.31±0.13	HD 263175 B	06:46:07.5	+32:33:15	8.99±0.02	M1.0 V	C
06523-0510	A				HD 50281 A	06:52:18.1	-05:10:25	5.01±0.25	K3.5 V	H
	Ba,Bb	WNO 17	58.84±0.17	180.22±0.16	HD 50281 B	06:52:18.1	-05:11:24	6.58±0.03	M2.0 V+	C
	C	TNN 6	51.18±0.35	188.98±0.45	J06521752-0511158	06:52:17.5	-05:11:16	13.97±0.36
07041+7514	A				HD 51067 A	07:04:03.9	+75:13:39	6.14±0.02	G0 V	H
	B	STF 973	12.58±0.08	31.83±0.53	HD 51067 B	07:04:05.7	+75:13:50	7.00±0.02	G5	H
	C	LDS 1642	61.01±0.08	17.30±0.12	LP 16-395	07:04:09.5	+75:14:37	11.18±0.02	M4.0 V	C*
07058+8337	A				HD 48974	07:05:49.9	+83:36:44	7.51±0.03	G5 V	H
	B	LDS 1640	296.70±0.09	296.99±0.01	LP 4-248	07:03:11.0	+83:38:59	11.11±0.02	M3.5	C
07191+6644	A				HD 55745 A	07:19:08.3	+66:44:23	6.72±0.02	F8 V	H
	B	HZG 4	8.47±0.11	35.16±1.06	HD 55745 B	07:19:09.2	+66:44:30	8.88±0.03	M0.0 V	C
07321-0853	A				HD 59984	07:32:05.8	-08:52:53	5.09±0.27	G0 V	H
	B	STF 1112	23.80±0.11	112.98±0.13	BD-08 1964B	07:32:07.3	-08:53:02	8.84±0.02	K5 V	C
07400-0336	A				V869 Mon	07:39:59.3	-03:35:51	5.49±0.03	K2 V	H
	B	BGH 3	57.96±0.10	112.68±0.05	HD 61606 B	07:40:02.9	-03:36:13	6.38±0.02	K7 V	...
	"C"	... ^j	3894.11±0.09	296.75±0.01	BD-02 2198	07:36:07.1	-03:06:39	6.79±0.03	M1.0 V	C
08082+2106	A				BD+21 1764A	08:08:13.2	+21:06:18	6.86±0.02	K7 V	H
	B	COU 91	10.62±0.10	146.49±0.15	BD+21 1764Ba, Bb	08:08:13.5	+21:06:08	7.34±0.02	M3.0V	C
08082+7155	A				HD 66171	08:08:10.5	+71:55:28	6.98±0.02	G2 V	H
	B	LDS 1667	49.33±0.11	256.48±0.15	LP 35-148	08:08:00.3	+71:55:17	10.88±0.02	M2.0 V	C*
08107-1348	A				18 Pup A	08:10:39.8	-13:47:57	4.14±0.23	F6.5 V	H
	Ba,Bb	LDS 204	97.23±0.11	239.30±2.90	18 Pup B	08:10:34.3	-13:48:51	8.28±0.02	M3.0 V+	C
	C	WFC 287	79.14±0.11	204.33±0.11	J08103760-1349096	08:10:37.6	-13:49:10	10.65±0.02
08110+7955	A				BD+80 245	08:11:06.2	+79:54:30	8.71±0.03	G0 IV	H
	B	LDS 1668	110.54±0.08	208.34±0.06	LP 17-109	08:10:46.2	+79:52:52	12.54±0.03	K5 V	C*
	C	PWS 3	121.10±0.08	325.24±0.01	J08103991+7956089	08:10:39.9	+79:56:09	11.37±0.03
	D	OSO 21	15.83±0.08	289.35±0.19	J08110051+7954346	08:11:00.5	+79:54:35	14.65±0.06

Table B1 – continued Basic properties of investigated systems and stars.

WDS	Comp.	Discoverer code	ρ [arcsec]	θ [deg]	Name ^a	α (J2000)	δ (J2000)	J^b [mag]	Spectral type	Obs. ^c
08138+6306	A				HD 67850	08:13:45.8	+63:06:14	7.17±0.02	G0 V	H
	B	LDS 2564	244.54±0.10	112.74±0.01	NLTT 19115	08:14:19.0	+63:04:40	9.91±0.02	M1.5 V	C
	C	RAO 60	249.36±0.10	109.32±0.01	J08142041+6304518	08:14:20.4	+63:04:52	14.38±0.03
08161+5706	A				HD 68638	08:16:06.3	+57:05:39	6.07±0.02	G8 V	H
	B	ENG 34	127.21±0.11	145.96±0.01	HD 237688	08:16:15.1	+57:03:54	8.34±0.02	F8	...
	C	BUP 113	226.89±0.11	150.14±0.01	J08162022+5702224 ^k	08:16:20.2	+57:02:23	10.34±0.03
	D	GIC 79	60.03±0.11	148.08±0.03	G 194-18	08:16:10.3	+57:04:48	10.56±0.02	M2.5 V	C*
08484+2042	A				HD 75076	08:48:24.0	+20:41:47	7.54±0.02	F8 V	H
	B	TOK 266	34.18±0.10	22.55±0.21	J08482492+2042188	08:48:24.9	+20:42:18	11.33±0.02	M1.5 V	C*
08492+0329	A				HD 75302	08:49:12.5	+03:29:05	6.24±0.02	G5 V	H
	B	LEP 33	159.38±0.13	285.20±0.03	LSPM J0849+0329W	08:49:02.3	+03:29:47	10.76±0.02	M4	...
08526+2820	A				ρ^01 Cnc A	08:52:35.8	+28:19:51	4.77±0.24	G8 V	H
	B	LDS 6219	84.61±0.17	127.96±0.02	ρ^01 Cnc B	08:52:40.8	+28:18:59	8.56±0.03	M4.5 V	C
09008+2347	A				HD 77052	09:00:49.3	+23:46:48	7.65±0.02	G2 V	H
	B	TOK 268	55.50±0.18	79.094±0.22	J09005322+2346586	09:00:53.2	+23:46:59	11.40±0.02	M2.5	C
09029+0600	A				BD+06 2091	09:02:51.3	+06:00:28	8.67±0.03	G0 V	H
	B	GWP 1132	105.48±0.11	15.86±0.08	LSPM J0902+0602	09:02:53.2	+06:02:10	11.26±0.02	M1.5 V	C
09058+5532	A				HD 77599	09:05:45.9	+55:31:44	6.84±0.03	G0 V	H
	B	LDS 3852	56.35±0.23	53.044±0.32	NLTT 20915	09:05:51.2	+55:32:18	11.49±0.02	M3.5 V	C
09152+2323	A				HD 79498	09:15:09.4	+23:22:32	6.85±0.02	G5 V	H
	B	BUP 127	60.03±0.08	170.74±0.07	BD+23 2063B	09:15:10.1	+23:21:33	9.14±0.02	M0.0 V	C
	C	STT 570	74.03±0.09	78.10±0.08	BD+23 2065	09:15:14.7	+23:22:48	8.51±0.03	G0	...
09211+6024	A				BD+61 1116	09:21:06.8	+60:24:11	7.36±0.02	K0 V	H
	B	LDS 1227	164.97±0.10	150.97±0.01	LP 91-22	09:21:17.7	+60:21:47	9.13±0.02	M1.5 V	C
09245+0621	AB				HD 81212 AB	09:24:28.6	+06:21:00	5.81±0.03	F5	H
	C	LDS 3888	122.33±0.17	325.24±0.02	LP 547-41	09:24:23.9	+06:22:42	10.60±0.03	M4.0 V	C
09327+2659	A				DX Leo	09:32:43.8	+26:59:19	5.58±0.02	G9 V	H
	B	LDS 3903	65.04±0.20	67.28±0.22	HD 82443 B	09:32:48.3	+26:59:44	10.36±0.02	M5.5 V	C
09353-1019	A				HD 83008	09:35:17.9	-10:18:51	8.04±0.03	K0 V	H
	B	LDS 6229	91.64±0.10	280.848±0.05	BD-09 2878	09:35:11.8	-10:18:34	9.08±0.04	K5 V	C
09361+3733	A				HD 82939	09:36:04.3	+37:33:10	6.88±0.02	G5 V	H
	B	SKF 254	162.28±0.16	121.49±0.02	MCC 549 Ba,Bb	09:36:15.9	+37:31:46	8.09±0.02	M0.0 V	C
09393+1319	A				HD 83509 Aa,Ab	09:39:17.2	+13:18:45	6.01±0.02	F7 V	H
	B	TOK 270	50.56±0.13	131.55±0.01	J09391981+1318118	09:39:19.8	+13:18:12	11.56±0.02	m1	...
10010+3155	A				20 LMi A	10:01:00.7	+31:55:25	4.27±0.33	G3 V	H
	B	RAG 7	134.11±0.17	278.46±0.06	20 LMi B	10:00:50.3	+31:55:46	10.26±0.02	M6.0 V	C
10172+2306	A				39 Leo A	10:17:14.6	+23:06:23	4.99±0.26	F8 V	H
	B	STT 523	7.75±0.14	298.75±0.41	39 Leo B	10:17:14.1	+23:06:27	8.36±0.03	M1	...
10306+5559	A				36 UMa A	10:30:37.6	+55:58:50	4.03±0.22	F8 V	H
	B	LDS 2863	122.85±0.32	302.92±0.04	36 UMa B	10:30:25.3	+55:59:57	6.12±0.02	K7 V	C
	C	ARN 4	241.05±0.32	291.16±0.04	TYC 3819-1188-1	10:30:10.8	+56:00:17	10.50±0.02
10504-1326	A				BD-12 3277	10:50:22.4	-13:26:07	8.40±0.03	G3 V	H
	B	LDS 4023	8.55±0.08	21.40±0.73	LP 731-61	10:50:22.7	-13:26:00	11.65±0.05	m:	...
	C	LDS 4023	150.80±0.08	92.20±0.03	LP 731-65	10:50:32.8	-13:26:13	11.09±0.02	M4	...
	D	ARN 73	118.78±0.08	82.03±0.05	BD-12 3278	10:50:30.5	-13:25:51	7.502±0.02
10507+5148	A				LZ UMa	10:50:40.3	+51:47:59	6.62±0.02	G5 V	H
	B	LDS 3019	178.24±0.10	186.17±0.04	GJ 3628	10:50:38.3	+51:45:02	9.83±0.02	M3.5 V	...
10585-1046	A				BD-10 3166	10:58:28.8	-10:46:13	8.61±0.03	K0 V	H
	B	LDS 4041	20.75±0.10	214.47±0.38	LP 731-76	10:58:28.0	-10:46:31	9.51±0.02	M5.0 V	C
11047-0413	A				HH Leo	11:04:41.5	-04:13:16	6.30±0.03	G8 V	H
	BC	STF 1506	11.55±0.11	221.35±0.79	HD 96064 BC	11:04:41.0	-04:13:25	7.27±0.02	M0.5 V+	C
11152+7329	A				HD 97584 A	11:15:11.9	+73:28:31	5.78±0.02	K4 V	H
	B	STF 1516	60.40±0.14	103.49±0.10	BD+74 456a	11:15:25.8	+73:28:17	5.26±0.28	M2	...
	C	STT 539	6.52±0.10	322.74±0.16	HD 97584 B	11:15:11.1	+73:28:36	7.88±0.02	M2.5 V	C
11214-2027	A				SZ Crt	11:21:26.6	-20:27:13	6.10±0.02	K7 V	H
	B	STN 22	4.06±0.10	344.44±0.94	HD 98712 B	11:21:26.6	-20:27:09	6.64±0.07	M2.5 V	C

Table B1 – continued Basic properties of investigated systems and stars.

WDS	Comp.	Discoverer code	ρ [arcsec]	θ [deg]	Name ^a	α (J2000)	δ (J2000)	J^b [mag]	Spectral type	Obs. ^c
11218+1811	A				HD 98736	11:21:49.3	+18:11:24	6.49±0.02	K0 V	H
	B	STF 1534	5.15±0.14	316.36±0.05	BD+19 2443B	11:21:49.1	+18:11:28	7.65±0.08	M0.0 V	C
11378+4150	A				BD+42 2230A	11:37:50.8	+41:49:32	8.38±0.03	G6 V	H
	B	LDS 5735	28.49±0.18	340.37±0.22	BD+42 2230B	11:37:49.9	+41:50:00	11.04±0.02	M2.0 V	C
	C	DAL 24	5.68±0.21	172.32±1.86	J11375084+4149269	11:37:50.8	+41:49:27	10.57
11403+0931	A				BD+10 2321	11:40:16.6	+09:30:44	8.05±0.02	K0 V	H
	B	LDS 4131	62.38±0.16	88.32±0.15	LP 493-31	11:40:20.8	+09:30:45	10.12±0.02	M1.5 V	C
11455+4740 ^l	A				HD 102158	11:45:30.5	+47:40:01	6.86±0.03	G2 V	H
	B	LEP 45	1176.09±0.16	72.42±0.01	G 122-46	11:47:21.7	+47:45:57	10.59±0.02	m2.5	...
11475+7702	A				HD 102326	11:47:30.3	+77:02:24	7.43±0.03	G8 IV	H
	B	LDS 1739	60.91±0.11	281.65±0.08	LP 20-89	11:47:12.7	+77:02:36	9.20±0.02	K7 V	C
11523+0957	A				HD 103112	11:52:20.9	+09:56:53	5.87±0.02	K0 IV	H
	B	LDS 4152	230.10±0.17	349.05±0.03	LP 493-64	11:52:17.9	+10:00:39	11.42±0.03	M4.0 V	C
12049+1729	A				HD 104923	12:04:57.0	+17:28:36	7.21±0.02	K0 V	H
	B	LEP 49	27.26±0.10	206.62±0.28	RX J1204.9+1728	12:04:56.1	+17:28:12	9.79±0.02	M3.5 V	C
12051+1933	A				BD+20 2678A	12:05:07.0	+19:33:16	8.31±0.02	G5 V	H
	B	GIC 103	117.20±0.17	144.07±0.02	BD+20 2678B	12:05:11.9	+19:31:41	11.19±0.02	m2:	...
12069+0548	A				HD 105219	12:06:56.5	+05:48:12	7.18±0.02	K0 V	H
	B	HJ 1210	6.98±0.40	115.73±1.64	BD+06 2551B	12:06:56.9	+05:48:09	8.58±0.04	K5 V	C
12089+2147	Aa,Ab				BD+22 2442	12:08:54.7	+21:47:19	8.14±0.02	G2 V+	H
	B	LDS 930	15.716±0.11	39.30±0.58	BD+22 2442B	12:08:55.4	+21:47:32	11.15±0.02	M0.5 V	C
12372+3545	A				BD+36 2288	12:37:13.7	+35:44:46	8.47±0.02	G5 V	H
	B	LEP 58	273.10±0.11	4.49±0.03	LSPM J1237+3549	12:37:15.5	+35:49:18	11.35±0.02	M1.5 V	C
12406+4017	A				HD 110279	12:40:37.4	+40:17:17	7.38±0.02	F8 :V	H
	B	HJ 2617	5.69±0.16	2.21±1.58	BD+41 2317B	12:40:37.4	+40:17:23	8.28±0.06	G:V	...
	C	HJ 2617	170.20±0.16	175.3±0.05	TYC 3021-982-1	12:40:38.5	+40:14:27	9.99±0.03	F:V	...
	D	BKO 114	43.44±0.16	343.70±0.14	J12403633+4017586	12:40:36.3	+40:17:59	10.61±0.02	M:	...
12482-2448	A				HD 111261 A	12:48:10.7	-24:48:24	6.80±0.02	K4 V	H
	B	HJ 4551	12.04±0.10	306.12±0.10	HD 111261 B	12:48:10.0	-24:48:16	7.32±0.03	K7 V	...
12489+1206	A				HD 111398	12:48:52.4	+12:05:47	5.90±0.02	G5 V	H
	B	ENG 49	173.43±0.13	349.15±0.03	TYC 885-572-1	12:48:50.2	+12:08:37	9.55±0.02
	C	ENG 49	300.30±0.13	340.17±0.01	BD+12 2516	12:48:45.4	+12:10:29	10.18±0.02	A0	...
	D	SLE 903	202.20±0.11	178.79±0.03	TYC 885-920-1	12:48:52.1	+12:02:25	10.10±0.02
	E	LEP 59	75.77±0.11	168.57±0.07	LSPM J1248+1204	12:48:53.5	+12:04:33	11.40±0.02	M4.5 V	C
12549-0620	A				BD-05 3596	12:54:56.0	-06:20:19	8.28±0.02	K5 V	H
	B	LDS 4294	20.14±0.23	318.56±0.06	GJ 488.2 B	12:54:55.1	-06:20:04	11.38±0.02	M4.5 V	C
13018+6337	A				HD 113337 A	13:01:46.9	+63:36:37	5.19±0.02	F5 V	H
	Ba,Bb	LDS 2662	119.79±0.14	307.44±0.012	LSPM J1301+6337	13:01:32.7	+63:37:50	10.31±0.02	M3.5+	...
13077-1411	A				HD 114001	13:07:39.2	-14:11:17	6.89±0.03	F5 V	H
	B	TOK 286	63.26±0.08	207.58±0.10	J13073714-1412130	13:07:37.1	-14:12:13	11.60±0.02	m3:	...
	C	TOK 286	1665.72±0.09	10.57±0.01	J13080016-1343595	13:08:00.2	-13:43:59	12.66±0.03
	D	GWP 1910	59.42±0.09	252.87±0.10	J13073525-1411344	13:07:35.3	-14:11:34	15.33±0.04
13114+0938	A				HD 114606 A	13:11:21.4	+09:37:34	7.53±0.02	G1 V	H
	B	LDS 5771	81.83±0.22	169.16±0.52	HD 114606 B	13:11:22.4	+09:36:13	9.68±0.02	M0.0 V	C
13169+1701	A				HD 115404 A	13:16:51.0	+17:01:02	4.90±0.04	K2 V	H
	B	BU 800	7.39±0.11	105.97±0.62	HD 115404 B	13:16:51.5	+17:01:00	6.53±0.03	M0.5 V	C
	C	BU 800	120.55±0.11	338.62±0.03	J13164800+1702543	13:16:48.0	+17:02:54	11.36±0.02
	D	BU 800	43.99±0.11	82.97±0.17	J13165410+1701074	13:16:54.1	+17:01:07	11.74±0.02
13253+4242	A				BD+43 2328	13:25:17.4	+42:41:58	7.87±0.02	K1 V	H
	B	TOK 288	72.77±0.16	112.81±0.06	StKM 1-1067	13:25:23.5	+42:41:30	9.08±0.02	K7 V	C
13274-2138	A				HD 116963	13:27:24.9	-21:39:19	7.94±0.02	K4 V	H
	B	LDS 6278	138.46±0.08	105.97±0.05	LP 797-105	13:27:34.5	-21:39:57	9.66±0.02	M2.5	...
13315-0800	A				HD 117579 A	13:31:28.7	-08:00:26	7.528±0.02	G5 V	H
	B	LDS 4371	31.51±0.10	31.00±0.24	HD 117579 B	13:31:29.8	-07:59:59	9.60±0.03	M0.0 V	C
13316+5857	A				HD 117845	13:31:33.8	+58:57:10	6.90±0.02	G2 V	H
	B	JNN 151	11.39±0.11	52.76±0.81	J13313493+5857171	13:31:34.9	+58:57:17	9.63±0.03	M1	...
	C	TOK 290	164.65±0.13	273.07±0.04	J13311250+5857191	13:31:12.5	+58:57:19	10.95±0.02	M2.5	C

Table B1 – continued Basic properties of investigated systems and stars.

WDS	Comp.	Discoverer code	ρ [arcsec]	θ [deg]	Name ^a	α (J2000)	δ (J2000)	J^b [mag]	Spectral type	Obs. ^c
13321-1115	Aa,Ab				HD 117676	13:32:04.7	-11:15:23	7.55±0.03	G8 V+	H
	B	TOK 291	83.98±0.13	157.60±0.05	TYC 5548-829-1	13:32:06.9	-11:16:41	9.45±0.03	M0.0 V	C
13470+0621	A				HD 120066	13:46:57.1	+06:21:01	5.21±0.02	G0 V	H
	B	LDS 3101	488.44±0.15	104.82±0.22	BD+07 2692	13:47:28.8	+06:18:56	7.76±0.04	K7 V	C
14050+0157	A				HD 122972	14:04:58.7	+01:56:59	7.51±0.03	G6 V	H
	B	LDS 5807	49.15±0.16	299.34±0.07	Ross 799	14:04:55.8	+01:57:23	10.13±0.02	M2	...
14196-0509	A				HD 125455 A	14:19:34.9	-05:09:04	6.09±0.03	K1 V	H
	B	KUI 67	15.08±0.21	105.17±0.58	HD 125455 B	14:19:35.9	-05:09:08	10.49±0.03	M4.0 V	C
14245+6015	A				BD+60 1536	14:24:26.9	+60:15:25	7.65±0.02	K5 V	H
	B	LDS 2710	8.79±0.13	153.91±0.39	LP 97-826	14:24:27.4	+60:15:17	9.73±0.02	M2.0 V	C
14252+5151	A				θ Boo A	14:25:11.8	+51:51:03	3.18±0.24	F7 V	H
	B	STT 580	69.46±0.30	181.62±0.25	θ Boo B	14:25:11.6	+51:49:54	7.88±0.02	M2.5 V	C
14255+2035	A				HD 126512	14:25:30.1	+20:35:25	6.08±0.04	F9 V	H
	B	LEP 67	63.11±0.09	289.67±0.05	LSPM J1425+203W	14:25:25.9	+20:35:46	12.46±0.03
14260+3422	A				BD+35 2558	14:25:59.9	+34:22:15	8.55±0.02	K0 V	H
	B	GIC 118	559.67±0.12	357.76±0.01	G 178-25	14:25:58.2	+34:31:34	10.38±0.02	K7 V	...
	C	PWS 7	31.01±0.13	286.28±0.16	J14255753+3422239 ^m	14:25:57.6	+34:22:24	13.06±0.03
	D	PWS 7	69.30±0.13	217.94±0.15	J14255649+3421205	14:25:56.5	+34:21:21	14.71±0.03
14336+0920	A				HD 127871 A	14:33:34.9	+09:20:04	7.16±0.02	K2 V	H
	B	LDS 962	73.49±0.21	85.501±0.17	HD 127871 B	14:33:39.9	+09:20:10	10.23±0.02	M3.5 V	C
14415+1336	A				HD 129290 A	14:41:28.7	+13:36:05	7.18±0.02	G2 V	H
	B	LDS 967	93.43±0.15	13.20±0.11	HD 129290 B	14:41:30.3	+13:37:36	10.35±0.02	M1.0 V	C
14446-2215	A				HD 129715	14:44:35.5	-22:15:11	7.23±0.02	K2 V	H
	B	LDS 4498	68.53±0.08	68.60±0.09	LP 858-23	14:44:40.1	-22:14:46	10.57±0.02	M4.5 V	C
14493+4950	AB				HD 130986 A	14:49:18.1	+49:50:16	6.94±0.02	F8 V+	H
	C	TOK 298	48.76±0.11	220.99±0.19	J14491476+4949390	14:49:14.8	+49:49:39	10.24±0.02	M1.5 V	C
14575-2125	A				HD 131977	14:57:28.0	-21:24:56	3.66±0.26	K4 V	H
	Ba,Bb	H N 28	24.68±0.41	305.15±0.23	HD 131976	14:57:26.5	-21:24:42	4.55±0.26	M1.5 V+	...
	C	H N 28	195.09±0.41	323.33±0.02	J14571953-2122161	14:57:19.5	-21:22:16	12.68±0.02	g:	...
	D	H N 28	259.75±0.30	343.74±0.04	J14572267-2120432	14:57:22.7	-21:20:43	12.61±0.02
	G	BUG 4	258.34±0.30	314.29±0.01	GJ 570 D	14:57:15.0	-21:21:48	15.32±0.05	T8	...
14595+4528	A				HD 132830	14:59:32.9	+45:27:51	7.09±0.02	K0 V	H
	B	DAM 30	63.11±0.11	202.93±0.14	MCC 56	14:59:30.6	+45:26:53	8.10±0.03	K7 V	C
15123+3939	A				HD 135144	15:12:17.8	+39:39:21	6.98±0.02	K3 V	H
	B	LEP 73	485.77±0.11	218.74±0.02	LP 222-50	15:11:51.5	+39:33:02	9.87±0.02	M2.5 V	C
15131+1808	A				BD+18 2985	15:13:06.9	+18:08:09	8.64±0.02	K0 V	H
	B	TOK 299	34.50±0.10	353.79±0.14	J15130664+1808438	15:13:06.6	+18:08:44	11.02±0.02	M2.0 V	C
15164+1648	A				HD 135792 A	15:16:25.6	+16:47:39	6.53±0.04	G0 V	H
	Ba,Bb	HO 547	5.32±0.10	292.50±0.56	HD 135792 B	15:16:25.3	+16:47:42	7.82±0.19	K5 V+	C
15204+0015	A				HD 136378	15:20:26.1	+00:14:41	7.77±0.03	K1 V	H
	B	GIC 126	196.55±0.11	170.51±0.03	Ross 1050	15:20:28.3	+00:11:27	9.45±0.03	M0.0 V	C
15211+2534	A				HD 136655	15:21:09.3	+25:34:02	7.31±0.04	K2 V	H
	B	GRV 903	69.05±0.08	243.04±0.09	MCC 739	15:21:04.8	+25:33:30	8.46±0.03	K7 V	C
15282-0921	Aa,Ab				HD 137763	15:28:09.6	-09:20:53	5.44±0.02	G9 V	H
	B	SHJ 202	52.25±0.11	132.64±0.01	HD 137778	15:28:12.2	-09:21:28	5.99±0.03	K2 V	H
	"C"	...	1216.24±0.10	342.62±0.01	GJ 586 C	15:27:45.1	-09:01:32	10.55±0.03	M4.5	C
15289+5727	A				HD 138367	15:28:51.9	+57:26:43	5.93±0.03	F7 V	H
	B	BU 945	35.50±0.11	97.02±0.16	J15285631+5726381	15:28:56.3	+57:26:38	11.38±0.02
	C	FOX 189	65.46±0.11	17.71±0.12	J15285442+5727448	15:28:54.4	+57:27:45	11.33±0.02
	D	GIC 128	185.26±0.11	130.64±0.01	G 224-69	15:29:09.4	+57:24:42	8.83±0.02	M1.0 V	C
15353+6005	A				HD 139477	15:35:20.0	+60:05:13	6.46±0.02	K3 V	H
	B	LDS 2723	42.33±0.24	97.27±0.28	LP 99-392	15:35:25.7	+60:05:08	9.27±0.02	M3.5 V	C*
15431-1303	A				HD 140269	15:43:08.7	-13:03:23	5.62±0.02	G1 V	H
	B	TOK 303	53.11±0.08	304.52±0.02	J15430573-1302525	15:43:05.7	-13:02:53	10.24±0.02	M1.5 V	C
15482+0134	A				V382 Ser	15:48:09.5	+01:34:18	5.99±0.02	G8 V	H
	B	EIS 1	17.83±0.11	352.42±0.29	HD 141272 B	15:48:09.3	+01:34:36	9.30±0.02	M2.5 V	C

Table B1 – continued Basic properties of investigated systems and stars.

WDS	Comp.	Discoverer code	ρ [arcsec]	θ [deg]	Name ^a	α (J2000)	δ (J2000)	J^b [mag]	Spectral type	Obs. ^c
22311+4509	A				HD 213519 A	22:31:05.7	+45:08:42	6.47±0.02	G5	H
	BC	LEP 108	62.24±0.08	7.62±0.08	HD 213519 B	22:31:06.5	+45:09:44	10.34±0.02	M3+	...
	D	RAO 29	61.58±0.09	354.10±0.08	J22310515+4509435	22:31:05.2	+45:09:44	14.97±0.04
22467+1210	A				ξ Peg A	22:46:41.6	+12:10:22	3.36±0.25	F6 V	H
	B	HJ 301	11.19±0.30	97.08±1.38	ξ Peg B	22:46:42.3	+12:10:21	7.94±0.02	M1.5	C*
	C	HJ 301	176.99±0.30	5.98±0.11	BPS CS 30332-0037	22:46:42.8	+12:13:19	11.73±0.02
22524+0950	A				σ Peg A	22:52:24.1	+09:50:08	4.23±0.29	F6 V	H
	Da,Db	LDS 6388	250.20±0.17	19.55±0.05	σ Peg B	22:52:29.8	+09:54:04	9.66±0.02	M3.0 V+	C
22589+6902	A				BD+68 1345A	22:58:53.8	+69:01:50	7.33±0.02	K0 V	H
	B	GIC 186	21.57±0.08	233.34±0.31	BD+68 1345B	22:58:50.6	+69:01:37	10.59±0.02	M3.0 V	C
23026+2948	A				BD+29 4841Aa,Ab	23:02:34.6	+29:48:18	7.24±0.02	K0 V	H
	B	TOK 352	45.34±0.10	248.51±0.16	J23023133+2948016	23:02:31.3	+29:48:02	11.12±0.02	M3.0 V	C*
	C	TOK 352	1294.97±0.09	144.190±0.001	J23033276+2930486	23:03:32.8	+29:30:49	11.92±0.02
23104+4901	A				HD 218790	23:10:21.3	+49:01:06	6.17±0.02	G0 V	H
	B	STF 2987	3.81±0.09	151.11±0.56	BD+48 3952B	23:10:21.5	+49:01:03	6.61±0.09	K5 V	C*
23194+7900	A				V368 Cep	23:19:26.6	+79:00:13	5.90±0.02	G9 V	H
	B	LDS 2035	10.85±0.11	215.14±0.78	HD 220140 B	23:19:24.5	+79:00:04	8.04±0.02	M3.5 V	C
	C	MKR 1	962.53±0.11	141.82±0.01	LP 12-90	23:22:53.9	+78:47:39	10.42±0.02	M5.0 V	C
23235+4548	A				HD 220445	23:23:28.8	+45:47:36	6.85±0.02	K0 V	H
	B	STF 3010	25.94±0.08	131.28±0.02	BD+44 4400	23:23:30.7	+45:47:19	7.38±0.02	K5 V	C
	C	STF 3010	38.69±0.08	129.06±0.02	J23233168+4547116	23:23:31.7	+45:47:12	11.10±0.02
23266+4520	Aa,Ab				HD 220821	23:26:40.6	+45:20:17	6.10±0.02	G0 V+	H
	B	GIC 192	54.30±0.10	332.99±0.05	J23263798+4521054	23:26:37.9	+45:21:05	5.93±0.02	MIII	C
	C	GIC 192	57.57±0.08	352.65±0.07	BD+44 4419B	23:26:39.6	+45:21:14	8.20±0.03	M4.5	...
23355+3101	A				HD 221830 A	23:35:28.9	+31:01:02	5.69±0.02	F9 V	H
	B	LDS 6405	8.04±0.09	114.04±0.97	HD 221830 B	23:35:29.5	+31:00:59	9.48±0.03	M2.5 V	C*
23419-0559	A				HD 222582 A	23:41:51.5	-05:59:09	6.52±0.02	G5 V	H
	Ba,Bb	LDS 5112	109.56±0.18	299.52±0.03	HD 222582 B	23:41:45.2	-05:58:15	10.39±0.02	M4.5 V+	C
23536+1207	A				MCC 870	23:53:35.5	+12:06:22	8.40±0.02	K4 V	H
	B	VYS 11	5.73±0.27	165.92±2.07	PM J23535+1206S	23:53:35.6	+12:06:17	8.67±0.03	M2.5 V	C*
23556+0042	A				HD 224157	23:55:36.0	+00:41:45	7.80±0.03	K0 V	H
	B	LEP 116	12.97±0.08	253.26±0.47	LSPM J2355+0041W	23:55:35.0	+00:41:41	9.93±0.02	M1.5 V	C*
23581+2420	A				HD 224459 Aa,Ab	23:58:03.9	+24:20:28	6.71±0.02	G2:	H
	B	STF 3048	8.66±0.10	313.33±0.03	BD+23 4830B	23:58:03.4	+24:20:33	8.24±0.02	K0 V	H
	C	STF 3048	38.00±0.10	260.90±0.17	TYC 2252-410-1	23:58:01.2	+24:20:22	10.55±0.02	G0	...
	D	LEP 118	619.21±0.11	144.42±0.01	G 131-6	23:58:30.2	+24:12:04	9.13±0.04	K7 V	C
	E	GIC 197	614.13±0.12	145.56±0.03	G 131-5	23:58:29.3	+24:12:02	10.63±0.02	M3 V	C*
	F	FYM 131	43.75±0.10	102.52±0.10	J23580699+2420185	23:58:06.7	+24:20:19	12.06±0.02
	G	FYM 131	81.91±0.10	119.95±0.03	J23580906+2419471	23:58:09.1	+24:19:47	11.62±0.02

^a Stars with Simbad name Jhhmmss±ddmmss are 2MASS stars (Skrutskie et al. 2006).

^b J magnitude values from 2MASS (Skrutskie et al. 2006).

^c Obs.: observed stars with HERMES (H) and CAFOS (C; Alonso-Floriano et al. 2015a; C*: unpublished).

^d Contrary to Simbad, it is not a spectroscopic binary (Goldin & Makarov 2007).

^e B component, unresolved by us, is GJ 105 C, an M7 V at $\rho = 1.7\text{--}3.3$ arcsec (Golimowski et al. 1995).

^f BD+50 860C in Simbad.

^g Equatorial coordinates and, therefore, ρ and θ are from raw H -band 2MASS images.

^h B component, unresolved by us, is 9 Aur B, an M2 V at $\rho = 4.5\text{--}6.3$ arcsec (Krisciunas et al. 1993).

ⁱ Discoverer code not available in WDS. System taken from Salim & Gould (2003).

^j Discoverer code not available in WDS. System taken from Poveda et al. (2009).

^k CCDM J08162+5705C in Simbad.

^l Pair rejected by proper motions in Caballero 2009 (note the wrong WDS identifier in his Table 2), but physical in WDS and this work.

^m CCDM J14260+3423C in Simbad.

ⁿ Discoverer code not available in WDS. System taken from Valls-Gabaud (1988).

^o B and C spectral types are switched in Simbad and literature.

^p WDS “D” component, LEP 96, points wrongly to a 2MASS artifact, which leads to considerable confusion in Simbad.

Table B2. Distances, proper motions, and remarks.

WDS	Name	d [pc]	Ref.	$\mu_\alpha \cos \delta$ [mas yr $^{-1}$]	μ_δ [mas yr $^{-1}$]	Ref.	Remarks
00153+5304	G 217-41	75.7 \pm 1.7	TGAS	+222.00 \pm 0.12	+45.89 \pm 0.10	TGAS	
	G 217-40	57.0 \pm 8.6	This work	+213.5 \pm 2.4	+55.5 \pm 2.4	HSOY	
00385+4300	BD+42 126	52.91 \pm 0.62	TGAS	+188.61 \pm 0.14	-81.45 \pm 0.14	TGAS	
	LP 193-345	77.3 \pm 6.2	This work	+194.00 \pm 8.00	-79.00 \pm 8.00	UCAC4	Wrong PPMXL μ
00452+0015	HD 4271 Aa,Ab	41.37 \pm 0.94	HIP2	+266.80 \pm 0.17	-51.19 \pm 0.17	HSOY	SB1
	HD 4271 B	24.1 \pm 4.9	This work	+265.6 \pm 1.9	-53.4 \pm 1.9	HSOY	WDS close
00467-0426	HD 4449	28.8 \pm 2.3	HIP2	+25.41 \pm 0.25	-260.99 \pm 0.25	HSOY	
	LP 646-9	39.7 \pm 8.1	This work	+23.1 \pm 2.2	-257 \pm 23	HSOY	
00491+5749	Achird Aa,Ab	5.95 \pm 0.02	HIP2	+1086.59 \pm 0.40	-559.43 \pm 0.33	HIP2	SB1
	η Cas B	Not enough information
	Zkh 17	-0.6 \pm 2.3	-4.6 \pm 2.3	HSOY	No common μ
01055+1523	HD 6440 A	27.26 \pm 0.19	TGAS	+7.99 \pm 0.14	-198.65 \pm 0.10	TGAS	
	HD 6440 B	19.40 \pm 0.52	This work	+6.30 \pm 0.68	-195.77 \pm 0.67	HSOY	
01076+2257	HD 6660 A	20.41 \pm 0.12	TGAS	+103.03 \pm 0.07	-490.27 \pm 0.05	TGAS	
	HD 6660 B	22.4 \pm 4.2	This work	+102.00 \pm 8.00	-492.00 \pm 8.00	UCAC4	
01187-0052	HD 7895	27.64 \pm 0.23	TGAS	+431.46 \pm 0.07	-252.07 \pm 0.05	TGAS	WDS close
	HD 7895 B	28.89 \pm 0.78	This work	+429.4 \pm 2.4	-258.6 \pm 3.8	UCAC4	
	J01184607-0048029	+32.9 \pm 2.2	+16.5 \pm 2.2	HSOY	No common μ
01215+3120	EN Psc	27.85 \pm 0.91	HIP2	+527.99 \pm 0.38	-120.46 \pm 0.41	HSOY	
	BD+30 206B	27.5 \pm 5.2	This work	+536.00 \pm 8.00	-120.00 \pm 8.00	UCAC4	
01226+1245	BD+12 168A	43.98 \pm 0.44	TGAS	+401.68 \pm 0.17	+9.89 \pm 0.13	TGAS	
	BD+12 168B	39.4 \pm 1.2	This work	+394.4 \pm 1.1	+15.2 \pm 1.1	This work	
01230-1258	HD 8389 A	29.87 \pm 0.22	TGAS	+462.00 \pm 0.06	-25.65 \pm 0.04	TGAS	
	HD 8389 B	20.8 \pm 1.3	This work	+457.48 \pm 0.67	-29.22 \pm 0.66	HSOY	WDS close
01340-0141	BD-02 247	83.4 \pm 3.0	TGAS	+172.96 \pm 0.11	-147.28 \pm 0.08	TGAS	
	LP 588-9	122 \pm 12	This work	+171.4 \pm 2.2	-149.6 \pm 2.2	HSOY	
01450-0104	BD-01 237	56.4 \pm 1.2	TGAS	+204.95 \pm 0.10	-55.83 \pm 0.07	TGAS	
	LP 588-44	72.1 \pm 9.6	This work	+203.4 \pm 2.1	-54.1 \pm 2.1	HSOY	
01572-1015	HD 11964 A	32.85 \pm 0.65	HIP2	-366.23 \pm 0.49	-242.39 \pm 0.49	HIP2	
	HD 11964 B	31.9 \pm 2.0	This work	-368.7 \pm 1.2	-247.0 \pm 1.1	UCAC5	
02290-1959	HD 15468	19.55 \pm 0.51	HIP2	+611.6 \pm 1.1	+238.9 \pm 1.2	HSOY	WDS close
	HD 15468 C	26.7 \pm 4.1	This work	+603.2 \pm 2.3	+230.4 \pm 2.3	HSOY	
02291+2252	BD+22 353Aa,Ab	51.05 \pm 0.57	TGAS	+181.87 \pm 0.18	-210.31 \pm 0.14	TGAS	SB1
	BD+22 353B	40.1 \pm 1.1	This work	+173.3 \pm 4.1	-205.1 \pm 5.5	This work	
	J02290160+2252084	+65.04 \pm 0.92	-4.70 \pm 0.92	HSOY	No common μ
	J02290400+2251573	+0.9 \pm 2.2	-6.1 \pm 2.2	HSOY	No common μ . No Simbad entry
02361+0653	HD 16160 A	7.18 \pm 0.02	HIP2	+1807.78 \pm 0.89	+1444.02 \pm 0.40	HIP2	
	BX Cet	6.7 \pm 1.4	This work	+1796.7 \pm 2.4	+1453.1 \pm 2.4	HSOY	
02442+4914	θ Per A	11.13 \pm 0.03	HIP2	+334.66 \pm 0.17	-89.99 \pm 0.17	HIP2	
	θ Per B	11.1 \pm 1.3	This work	+331 \pm 53	-72 \pm 33	This work	
	J02440341+4912590	-0.86 \pm 0.96	-1.07 \pm 0.96	HSOY	No common μ
02482+2704	BC Ari Aa,Ab	22.88 \pm 0.23	TGAS	+278.51 \pm 0.08	-120.88 \pm 0.04	TGAS	SB1
	LP 354-414	20.5 \pm 4.9	This work	+275.00 \pm 8.00	-123.00 \pm 8.00	UCAC4	
02556+2652	HD 18143 A	22.55 \pm 0.12	TGAS	+265.09 \pm 0.10	-192.85 \pm 0.05	TGAS	
	HD 18143 B	17.27 \pm 0.52	This work	+280.17 \pm 0.87	-167.5 \pm 1.7	This work	
	HD 18143 C	18.7 \pm 3.8	This work	+251.3 \pm 1.0	-177.1 \pm 1.0	HSOY	
03042+6142	HD 18757	23.40 \pm 0.18	TGAS	+721.89 \pm 0.03	-693.61 \pm 0.03	TGAS	
	J03040397+6142596	+5.8 \pm 1.5	+1.8 \pm 1.5	HSOY	No common μ
	vMa 2-4	19.8 \pm 3.4	This work	+717.7 \pm 2.4	-697.8 \pm 2.4	HSOY	
03078+2533	HD 19381 A	66.8 \pm 1.3	TGAS	-8.65 \pm 0.06	-99.27 \pm 0.05	TGAS	
	HD 19381 B	49.5 \pm 9.3	This work	-9.4 \pm 2.2	-100.8 \pm 2.2	HSOY	
03150+0101	BD+00 549A	75.2 \pm 1.4	TGAS	+362.29 \pm 0.17	+116.28 \pm 0.11	TGAS	
	BD+00 549B	130 \pm 10	This work	+360.4 \pm 2.1	+115.0 \pm 2.2	HSOY	
03206+0902	HD 20727 Aa,Ab	44.3 \pm 1.0	TGAS	+288.36 \pm 0.07	-62.62 \pm 0.05	TGAS	SB1
	HD 20727 B	37.6 \pm 7.7	This work	+290.8 \pm 2.3	-62.5 \pm 2.3	HSOY	

Table B2 – continued Distances, proper motions, and remarks.

WDS	Name	d [pc]	Ref.	$\mu_\alpha \cos \delta$ [mas yr $^{-1}$]	μ_δ [mas yr $^{-1}$]	Ref.	Remarks
03321+4340	HD 21727 A	54.50 \pm 0.74	TGAS	+298.57 \pm 0.12	-119.53 \pm 0.09	TGAS	
	HD 21727 B	50.8 \pm 1.4	This work	+299.00 \pm 8.00	-119.00 \pm 8.00	UCAC4	
03332+4615	V577 Per	36.30 \pm 0.32	TGAS	+68.59 \pm 0.09	-175.38 \pm 0.06	TGAS	
	HD 21845 B	31.4 \pm 2.0	This work	+64.7 \pm 4.0	-172.4 \pm 3.6	UCAC4	
03356+4253	HD 22122	68.2 \pm 1.4	TGAS	+147.44 \pm 0.37	-155.06 \pm 0.35	TGAS	
	J03353356+4252364	-1.7 \pm 2.2	-3.3 \pm 2.2	HSOY	No common μ
	HD 22157	235 \pm 16	TGAS	+3.95 \pm 0.05	-26.09 \pm 0.04	TGAS	No common μ, d
	Wolf 191	90.5 \pm 7.2	This work	+141.2 \pm 1.6	-155.8 \pm 1.6	HSOY	
03396+1823	V1082 Tau Aa,Ab	36.40 \pm 0.30	TGAS	+187.81 \pm 0.12	-192.33 \pm 0.08	TGAS	SB2
	J03393295+1823017	+174	-195	This work	
	Wolf 209	37.4 \pm 4.3	This work	+189.2 \pm 2.4	-192.7 \pm 2.4	HSOY	SB2
03398+3328	HD 278874 Aa,Ab	39.00 \pm 0.53	TGAS	-36.19 \pm 0.10	-2.57 \pm 0.06	TGAS	SB2 (New)
	HD 278874 B	20.7 \pm 3.5	This work	-37.9 \pm 1.7	-4.9 \pm 4.3	This work	
03480+4032	HD 23596	52.16 \pm 0.73	TGAS	+53.38 \pm 0.04	+21.86 \pm 0.03	TGAS	
	J03480588+4032226	37.8 \pm 4.4	This work	+55.5 \pm 1.7	+20.7 \pm 1.7	HSOY	
03520+3947	HD 275867	32.10 \pm 0.26	TGAS	+33.41 \pm 0.11	-52.29 \pm 0.08	TGAS	
	TYC 2868-639-1	31.92 \pm 0.24	TGAS	+26.70 \pm 0.89	-57.30 \pm 0.46	TGAS	
03556+5214	HD 24421	39.3 \pm 1.1	TGAS	-119.89 \pm 0.04	+108.85 \pm 0.03	TGAS	
	LSPM J0355+5214	58.6 \pm 8.9	This work	-121.6 \pm 4.0	+112.50 \pm 0.51	This work	
	LSPM J0355+5209	-121.8 \pm 1.4	+107.27 \pm 0.51	UCAC4	
03566+5042	43 Per Aa,Ab	37.4 \pm 1.2	HIP2	+92.0 \pm 1.1	-128.47 \pm 0.93	HIP2	SB2
	BD+50 860B	37.92 \pm 0.35	TGAS	+90.7 \pm 1.3	-129.84 \pm 0.70	TGAS	
	J03564340+5040438	+1.6 \pm 2.3	-0.1 \pm 2.3	HSOY	No common μ
	J03562999+5042055	-1.8 \pm 2.3	-1.5 \pm 2.3	HSOY	No common μ . No Simbad entry
03575-0110	HD 24916 A	15.26 \pm 0.06	TGAS	-185.89 \pm 0.08	-143.32 \pm 0.06	TGAS	
	HD 24916 B	14.0 \pm 2.1	This work	-182.4 \pm 8.0	-139.1 \pm 4.0	UCAC4	
04153-0739	σ^2 Eri A	4.99 \pm 0.01	HIP2	-2240.12 \pm 0.23	-3420.27 \pm 0.20	HIP2	
	σ^2 Eri B	5.04	...	-2214.0 \pm 7.4	-3384.9 \pm 5.0	This work	
	σ^2 Eri C	4.13 \pm 0.92	This work	-2366 \pm 28	-3336 \pm 14	This work	
04252+2545	HD 27887 A	65.2 \pm 1.4	TGAS	+58.43 \pm 0.07	-24.14 \pm 0.04	TGAS	
	HD 27887 B	90 \pm 12	This work	+51.4 \pm 2.6	-20.7 \pm 2.6	HSOY	
04359+1631	Aldebaran	20.43 \pm 0.32	HIP2	+63.45 \pm 0.84	-188.94 \pm 0.65	HIP2	
	Aldebaran B	+63	-189	Iva08	
	BD+16 630	23.5 \pm 6.6	vAl95	+86.6 \pm 1.0	-23.6 \pm 1.0	HSOY	No common μ
04397+0952	HD 286955	30.6 \pm 1.4	HIP2	-14.99 \pm 0.51	-373.62 \pm 0.58	HSOY	WDS close
	BD+09 621B	37.5 \pm 6.3	This work	-24.3 \pm 2.5	-366.1 \pm 2.5	HSOY	
04429+1843	HD 29836	42.09 \pm 0.62	TGAS	+103.74 \pm 0.06	-91.23 \pm 0.04	TGAS	
	HD 285970	44.23 \pm 0.96	TGAS	+102.19 \pm 0.16	-94.19 \pm 0.09	TGAS	
	LP 415-358	+148.4 \pm 2.3	-116.8 \pm 2.3	HSOY	No common μ
04559+0440	HD 31412	37.27 \pm 0.63	TGAS	+138.85 \pm 0.04	-188.19 \pm 0.02	TGAS	WDS close
	HD 31412 B	22.5 \pm 3.0	This work	+136.0 \pm 8.0	-185.0 \pm 8.0	UCAC4	
05003+2508	HD 31867 A	39.75 \pm 0.44	TGAS	+61.73 \pm 0.09	+4.88 \pm 0.07	TGAS	
	HD 31867 B	43.1 \pm 4.2	This work	+68.5 \pm 5.9	+4.9 \pm 5.9	UCAC4	
05067+5136	9 Aur Aa,Ab	26.29 \pm 0.23	HIP2	-29.06 \pm 0.14	-172.37 \pm 0.18	HSOY	SB1
	9 Aur C	21.49 \pm 0.35	This work	-27.6 \pm 1.3	-171.5 \pm 1.3	HSOY	
	J05063820+5138136	+3.8 \pm 2.5	-3.0 \pm 2.5	HSOY	No common μ
05189-2124	HD 34751 A	20.33 \pm 0.20	TGAS	-137.94 \pm 0.06	-37.04 \pm 0.07	TGAS	
	HD 34751 B	10.3 \pm 2.1	This work	-134	-47	This work	
05264+0351	HD 35638	62.0 \pm 1.0	TGAS	+52.40 \pm 0.07	+37.39 \pm 0.04	TGAS	
	J05262029+0351111	78.1 \pm 9.0	This work	+48.7 \pm 2.3	+35.6 \pm 2.3	HSOY	No Simbad entry
05289+1233	HD 35956 Aa,Ab	28.17 \pm 0.75	HIP2	+91.62 \pm 0.17	-214.40 \pm 0.17	HSOY	SB1
	J05285199+1233049	+98	-189	This work	No Simbad entry
	J05285166+1233117	+14	+20	This work	No common μ . No Simbad entry
	J05285058+1232560	+9.1 \pm 2.3	-7.4 \pm 2.4	UCAC5	No common μ . No Simbad entry
	G 102-4	19.5 \pm 4.0	This work	+95.1 \pm 2.5	-215.2 \pm 2.5	HSOY	

Table B2 – continued Distances, proper motions, and remarks.

WDS	Name	d [pc]	Ref.	$\mu_\alpha \cos \delta$ [mas yr $^{-1}$]	μ_δ [mas yr $^{-1}$]	Ref.	Remarks
05413+5329	V538 Aur	12.28±0.08	HIP2	+1.82±0.48	-523.99±0.31	HIP2	
	HD 233153	12.44±0.26	HIP2	+3.38±0.99	-515.2±1.2	HSOY	
	J05411251+5330239	-6.5±2.2	-2.0±2.2	HSOY	No common μ
	HD 37229	+8.49±0.32	-32.41±0.41	HSOY	No common μ
05427+0241	HD 38014	32.39±0.33	TGAS	+253.82±0.09	-526.59±0.07	TGAS	
	G 99-27	25.8±4.4	This work	+243.8±2.3	-530.6±2.4	HSOY	
05445-2227	γ Lep	8.93±0.01	HIP2	-291.67±0.14	-368.97±0.15	HIP2	
	AK Lep	9.00±0.37	HIP1	-304.4±1.0	-352.2±1.0	TYC	
	J05442769-2223272	6.7±1.1	10.9±1.1	HSOY	No common μ
	vB 1	46.7±8.7	This work	-253.1±3.8	-591.1±3.7	HSOY	No common μ, d . No WDS entry
05466+0110	HD 38529 A	39.28±0.62	HIP2	-79.12±0.48	-141.84±0.35	HIP2	
	HD 38529 B	34.2±5.2	This work	-77.6±2.3	-142.6±2.3	HSOY	
05584-0439	HD 40397 A	24.46±0.14	TGAS	+73.65±0.05	-202.19±0.04	TGAS	WDS close
	HD 40374	87±13	TGAS	+15.7±1.3	+48.8±1.2	TGAS	No common μ, d
	LP 659-4	30.9±6.9	This work	+79.5±2.2	-215.3±2.2	HSOY	
06066+0431	Ross 413	58.41±0.89	TGAS	+154.34±0.25	-790.14±0.17	TGAS	
	vB 2	56.6±9.6	This work	+155.0±8.0	-790.0±8.0	UCAC4	
06173+0506	HD 43587	19.25±0.15	HIP2	-187.72±0.37	+170.69±0.28	HIP2	WDS close and SB1
	HD 254595	306±26	TGAS	-7.03±0.92	+2.32±0.88	TGAS	No common μ, d
	J06171345+0505419	-0.9±1.0	-4.8±1.0	HSOY	No common μ
	J06171372+0505030	+2.0±1.0	-10.4±1.2	HSOY	No common μ
	G 106-36	18.3±3.4	This work	-207.4±2.4	+168.4±2.4	HSOY	WDS close
06314-0134	HD 291763	52.25±0.71	TGAS	-247.22±0.15	-345.49±0.11	TGAS	
	LHS 6107	65.55±7.57	This work	-250.5±5.5	-320.9±5.5	PPMXL	
06319+0039	HD 291725	72.8±1.7	TGAS	-234.65±0.08	-77.34±0.07	TGAS	
	NLTT 16628	83.5±9.6	This work	-234.4±2.2	-74.2±2.3	HSOY	
06332+0528	HD 46375 A	34.8±1.1	HIP2	+111.96±0.88	-97.17±0.88	HIP2	
	HD 46375 B	24.7±3.3	This work	+112.2±1.3	-97.7±1.3	UCAC4	
06368+3751	BD+37 1545	64.4±1.0	TGAS	-60.95±0.16	-226.56±0.16	TGAS	
	LSPM J0636+3751W	54±10	This work	-44.0±8.0	-222.0±8.0	UCAC4	
06461+3233	HD 263175 A	25.25±0.29	TGAS	-455.91±0.23	+99.50±0.25	TGAS	
	HD 263175 B	35.6±3.5	This work	-463.5±1.1	+104.4±1.1	UCAC5	
06523-0510	HD 50281 A	8.71±0.03	HIP2	-544.14±0.44	-3.32±0.34	HIP2	
	HD 50281 B	9.3±1.2	This work	-576.7±2.9	-11.6±1.0	This work	Wrong Simbad μ . WDS close
	J06521752-0511158	-3.9±3.0	-5.8±4.6	UCAC5	No common μ . No Simbad entry
07041+7514	HD 51067 A	38.10±0.45	TGAS	-91.07±0.08	-256.53±0.10	TGAS	
	HD 51067 B	39.37±0.36	TGAS	-85.83±0.20	-254.72±0.26	TGAS	
	LP 16-395	39.3±8.1	This work	-85.5±2.3	-253.4±2.3	HSOY	
07058+8337	HD 48974	51.71±0.67	TGAS	+26.01±0.06	-221.12±0.07	TGAS	
	LP 4-248	46.5±8.7	This work	+28.0±2.3	-223.0±2.3	HSOY	
07191+6644	HD 55745 A	52.16±0.73	TGAS	-82.98±0.05	-151.80±0.05	TGAS	
	HD 55745 B	39.6±2.5	This work	-84.7±2.5	-153.5±2.5	UCAC4	
07321-0853	HD 59984	27.92±0.42	HIP2	-92.03±0.55	-167.86±0.35	HIP2	
	BD-08 1964B	29.61±0.40	This work	-111±24	-182±24	UCAC5	
07400-0336	V869 Mon	14.08±0.08	TGAS	+70.16±0.04	-278.14±0.02	TGAS	
	HD 61606 B	14.05±0.07	TGAS	+66.64±0.73	-286.58±0.60	TGAS	
	BD-02 2198	14.30±0.16	TGAS	+57.72±0.09	-275.89±0.05	TGAS	No WDS entry
08082+2106	BD+21 1764A	17.81±0.08	TGAS	-297.22±0.15	-354.99±0.11	TGAS	
	BD+21 1764Ba, Bb	9.8±1.7	This work	-273.2±1.1	-348.0±1.1	HSOY	
08082+7155	HD 66171	47.04±0.55	TGAS	-237.53±0.05	-447.89±0.06	TGAS	
	LP 35-148	67.3±9.0	This work	-242.0±2.2	-449.4±2.2	HSOY	
08107-1348	18 Pup A	22.50±0.47	TGAS	-251.04±0.03	+58.20±0.02	TGAS	
	18 Pup B	15.0±2.5	This work	-241.6±2.5	+53.6±2.5	HSOY	WDS close
	J08103760-1349096	-21.7±1.1	+13.75±0.94	HSOY	No common μ . No Simbad entry
08110+7955	BD+80 245	248±13	TGAS	+136.73±0.12	-367.50±0.12	TGAS	
	LP 17-109	235.9±4.1	This work	+135.4±2.3	-366.0±2.3	HSOY	
	J08103991+7956089	-5.8±2.3	+21.3±2.5	HSOY	No common μ
	J08110051+7954346	-9.2±3.2	-11.6±3.1	HSOY	No common μ

Table B4 – continued Abundances [X/H] with respect to the Sun for the four α -elements (Mg, Si, Ca and Ti), the Fe-peak elements (Cr, Mn, Co, and Ni), and the odd-Z elements (Na, Al, Sc, and V).

WDS	Name	[Na/H]	[Mg/H]	[Al/H]	[Si/H]	[Ca/H]	[Sc/H]	[Ti/H]	[V/H]	[Cr/H]	[Mn/H]	[Co/H]	[Ni/H]
22589+6902	BD+68 1345A	-0.19±0.04	-0.09±0.04	-0.02±0.02	-0.07±0.03	-0.15±0.06	-0.08±0.07	0.03±0.05	0.11±0.08	-0.08±0.04	-0.20±0.05	-0.04±0.03	-0.13±0.03
23026+2948	BD+29 4841 Aa,Ab
23104+4901	HD 218790	0.37±0.02	0.29±0.03	0.29±0.01	0.27±0.03	0.21±0.02	0.37±0.04	0.30±0.02	0.34±0.03	0.29±0.02	0.26±0.03	0.33±0.02	0.30±0.02
23194+7900	V368 Cep
23235+4548	HD 220445	0.03±0.10	-0.08±0.04	0.15±0.06	0.04±0.04	0.06±0.12	0.24±0.15	0.23±0.13	0.52±0.16	0.04±0.09	-0.05±0.11	0.12±0.06	-0.01±0.05
23266+4520	HD 220821	-0.21±0.02	-0.21±0.04	-0.11±0.02	-0.20±0.02	-0.13±0.04	-0.08±0.04	-0.10±0.03	-0.13±0.04	-0.18±0.02	-0.36±0.06	-0.25±0.04	-0.25±0.02
23355+3101	HD 221830 A	-0.39±0.01	-0.21±0.02	-0.15±0.01	-0.22±0.03	-0.22±0.03	-0.20±0.10	-0.11±0.02	-0.25±0.03	-0.39±0.02	-0.78±0.06	-0.30±0.03	-0.40±0.02
23419-0559	HD 222582 A	-0.06±0.03	-0.04±0.02	0.03±0.02	0.01±0.02	-0.05±0.04	-0.02±0.03	0.02±0.03	-0.01±0.03	0.05±0.03	-0.06±0.05	0.02±0.02	-0.04±0.02
23536+1207	MCC 870	0.05±0.37	-0.70±0.08	0.11±0.18	-0.65±0.21	...	0.72±0.38	0.24±0.34	0.57±0.38	...	-0.66±0.22	-0.20±0.17	-0.48±0.13
23556+0042	HD 224157	0.02±0.08	0.06±0.04	0.07±0.03	0.06±0.04	-0.01±0.06	0.07±0.07	0.16±0.06	0.31±0.09	0.10±0.05	-0.03±0.07	0.11±0.03	-0.02±0.03
23581+2420	HD 224459 Aa,Ab
	BD+23 4830B	-0.12±0.02	-0.15±0.05	-0.02±0.03	-0.07±0.02	-0.10±0.05	-0.05±0.05	0.03±0.04	0.09±0.07	-0.03±0.04	-0.08±0.06	-0.05±0.02	-0.11±0.02

Table B5 – continued Kinematics of late-F-, G-, and late-K stars.

WDS	Name	V_r [km s $^{-1}$]	U [km s $^{-1}$]	V [km s $^{-1}$]	W [km s $^{-1}$]	Pop. ^b	SKG ^c	SKG _{lit}	Ref. ^d
22589+6902	BD+68 1345A	-33.08±0.14	-105.8±3.1	-81.3±1.4	-1.10±0.14	TD	×
23026+2948	BD+29 4841Aa,Ab ^a	-7.09±0.25	23.74±0.75	2.34±0.35	14.8±0.39	D	×
23104+4901	HD 218790	-4.85±0.06	-47.32±0.51	-20.69±0.18	-8.38±0.10	D	HS	Field	BAN Σ
23194+7900	V368 Cep	-16.8±2.0	-9.48±0.91	-23.2±1.7	-5.46±0.58	D	LA	LA	Mon01
23235+4548	HD 220445	-49.43±0.22	-4.67±0.47	-53.83±0.28	3.98±0.21	D	×
23266+4520	HD 220821	-2.50±0.07	-70.0±2.0	-26.85±0.71	-6.50±0.21	D	×
23355+3101	HD 221830 A	-112.24±0.04	-66.7±1.5	-113.45±0.31	62.92±0.15	TD	×
23419-0559	HD 222582 A	11.89±0.02	37.01±0.46	-0.73±0.08	-11.01±0.02	D	×
23536+1207	MCC 870	-22.07±0.36	6.08±0.08	-30.34±0.37	2.01±0.37	D	×
23556+0042	HD 224157	26.31±0.15	-44.3±4.0	-8.2±2.0	-33.3±1.0	D	×
23581+2420	HD 224459 Aa,Ab ^a	-11.59±0.05	37.9±1.3	-26.78±0.68	-30.0±1.4	D	×
	BD+23 4830B	-12.01±0.14	38.2±1.4	-28.08±0.74	-31.0±1.5	D	×

^a Systemic radial velocity of spectroscopic binaries taken from references in Table 2.

^b Population – D: Thin Disc; D-TD: Thin/Thick Disc; H: Halo; TD: Thick Disc.

^c Stellar Kinematic Group – ×: No young disc; YD: Young disc; Cas: Castor; HS: Hyades SC; IC: IC2391 SC; LA: Local Association; UMa: Ursa Major MG; ; C-N: Carina-Near according to BANYAN Σ ; Field: not associated to any SKG according to BANYAN Σ .

^d SKG Reference – BAN Σ : [Gagné et al. \(2018\)](#); Eis13: [Eisenbeiss et al. \(2013\)](#); Fuh04: [Fuhrmann \(2004\)](#); Rie17: [Riedel et al. \(2017\)](#); Mon01: [Montes et al. \(2001\)](#); Tab12: [Tabernero et al. \(2012\)](#); Tab17: [Tabernero et al. \(2017\)](#).

This paper has been typeset from a $\text{\TeX}/\text{\LaTeX}$ file prepared by the author.